



He effects in concentrated equiatomic refractory alloys with increasing chemical complexity: From medium to high entropy alloys (HeRHEA)

> **EUROFUSION ENR-MAT.02.VTT-T002-D001** $01/01/2024 \longrightarrow 31/12/2025$

> > PI: Prof.Flyura Djurabekova



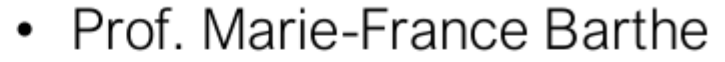
Partners of the HeRHEA project

VTT:



- Prof. Flyura Djurabekova (UHEL) – Pl of HerHEA project
- Prof. Filip Tuomisto (UHEL)
- Dr Kenichiro Mizohata (UHEL)
- Dr. Jesper Byggmästar (UHEL)
- Dr. Guanying Wei (UHEL)
- MSc Zhehao Chen (UHEL)
- BSc Toni Sutinen (UHEL)
- Dr Tomi Suhonen (VTT)
- Dr. Goel Sneha (VTT)

CEA:





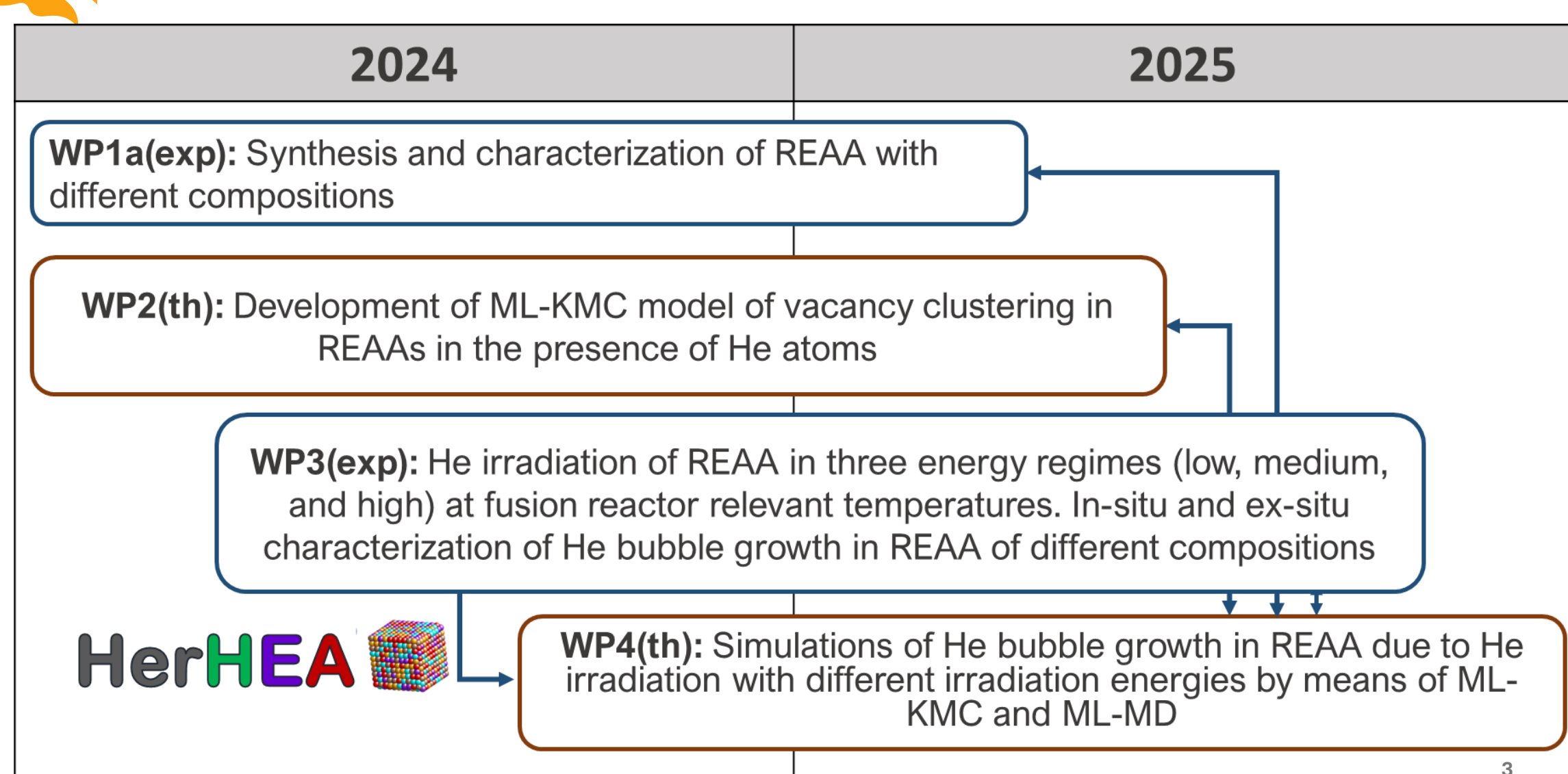
- Dr. Pierre Desgargin
- Dr. Thierry Sauvage
- Dr. Z Hu
- Dr. J. Joseph
- Dr. O. Wendling
- Dr. F. Foucher
- Dr. C. Genevois
- Dr. Stéphanie Jublot-Leclerc
- Dr. Antoine Combrisson
- Dr. Aurélie Gentils







Timeline of HeRHEA project





WP1(exp) "Synthesis and characterization of REAA with different compositions"



Samples



Material fabrication at VTT
Available material(s) to be studied
W, W-Ta, W-Mo, W-V

Other materials from Portugal W-Ta-V, W-Ta-Mo

Cutting of the bulk asfabricated material

subcontractor in France for EDM cutting

Electrical Discharge Machining

squares s

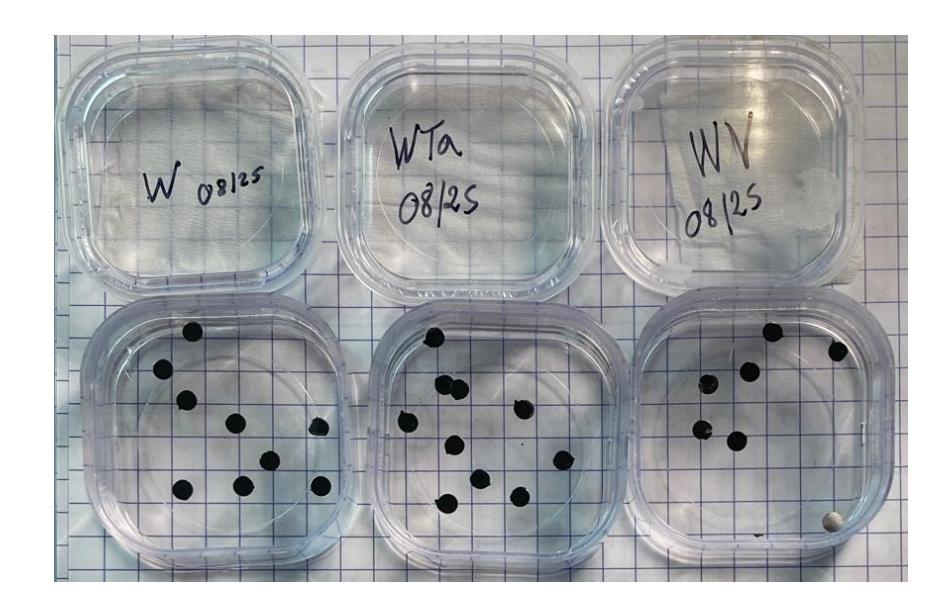
Materials sent to CNRS-CEMHTI and UHEL for ex situ ion implantation and characterizations



half discs

Quick SEM-EDX characterization of binary alloys

Surface mechanical polishing





Polishing performed on W, W-V, W-Ta and the ternary alloys WTaV, WTaMo

Mirror-polished samples (mid August / Sept.)

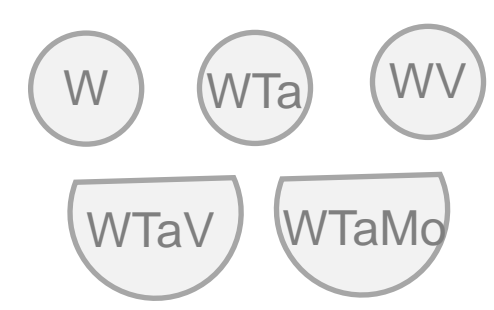


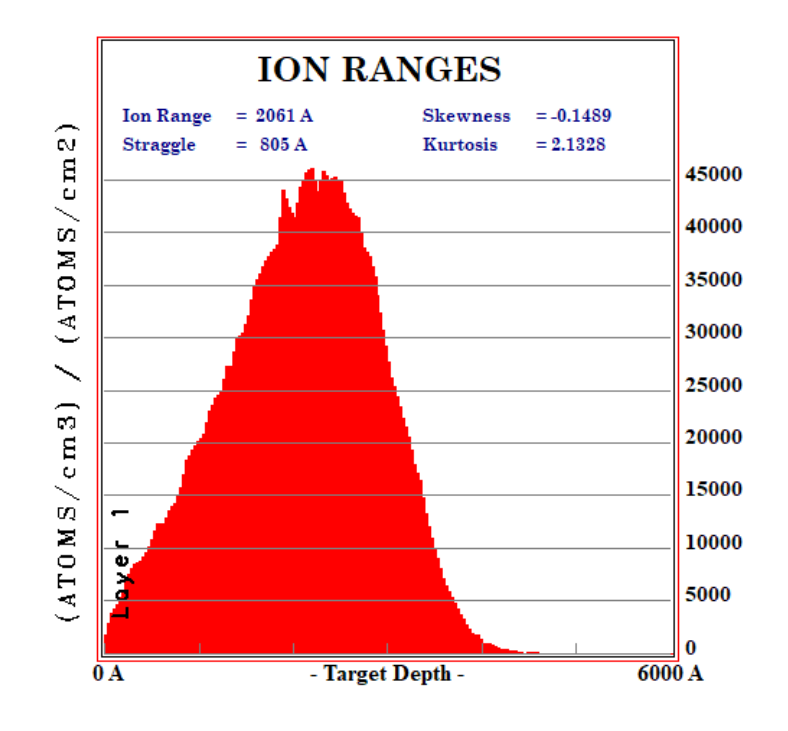
Samples



Ion implantation performed in Sept. 2025 using 190 kV IRMA ion implanter

He energy: 100 keV
He fluence: 1x10¹⁷ cm⁻²
Temperature of the samples: 500°C







Samples attached on the implantation sample holder

From literature: should be enough He to see bubbles in W

- □ SRIM calculations using average Ed = 44 eV, see J. Byggmästar, F. Djurabekova, and K. Nordlund, Phys. Rev. Materials 8 (2024) 115406
- □ He bubbles observed in W by TEM starting 5x10¹⁵ cm⁻² fluence (12 keV, 600°C), see F. Luo *et al*, Fusion Engineering and Design **125** (2017) 463, dx.doi.org/10.1016/j.fusengdes.2017.04.014



WP2(th) "Development of ML-KMC model of vacancy clustering in REAAs in the presence of He atoms"

Diffusion of helium in tungsten-based refractory alloys by molecular dynamics simulations



Potential He-refractory alloys



$$f(r_{ij}) = \begin{cases} \text{ZBL}, & r_{ij} \le r_1, \\ e^{b_0 + b_1 r_{ij} + b_2 r_{ij}^2 + b_3 r_{ij}^3}, & r_1 \le r_{ij} \le r_2, \\ \sum_{n=1}^{12} a_n (r_n - r_{ij})^3 H(r_n - r_{ij}), & r_{ij} \ge r_2, \end{cases}$$
(1)

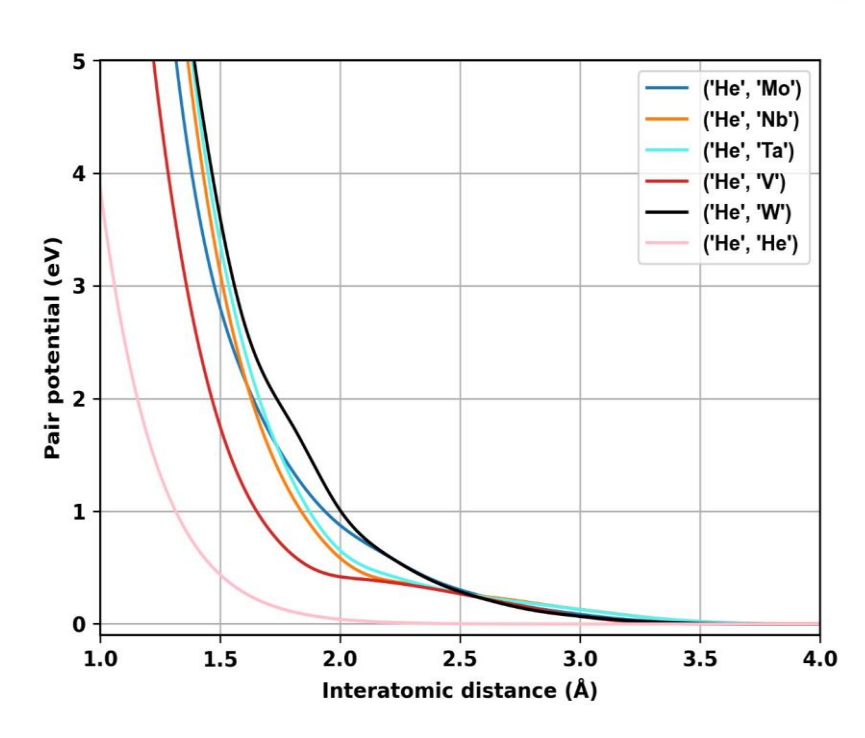


Table 2: Properties used for fitting and testing the interaction between refractory metals and He. Tetra. and Octa. means the formation energy of a He at the tetrahedral and octahedral positions. Reference values are from the corresponding DFT, ab-initio and MD calculations. All the units are eV.

W-He	Present value	Reference values	Мо-Не	Present value	Reference values
Tetra.	6.18	6.15, 9, 24, 6.16, 4, 13, 6.22, 25, 16, 6.23, 6.23	Tetra.	5.33	$5.16^{27}, 5.28^{28}, 5.31^{18}, 5.33^{29}$
Octa.	6.34	6.31 6.34 6.37 9.24 6.38 6.44 6.44 6.48	Octa.	5.44	5.33^{27} , 5.45^{28} , 5.48^{29} , 5.49^{18}
E_{binding}	4.76	4.57^{914} , 4.62^{26} , 4.63^{25} , 4.75^{18} , 4.91^{16}	$E_{\rm binding}$	3.65	$3.64^{28}, 3.65^{18}, 3.66^{29}, 3.67^{27}$
$E_{\rm mig}$	0.09	0.06 4 18 ,0.07 25 26 ,0.09 16	$E_{\rm mig}$	0.09	0.06 18
Ta-He	Present value	Reference values	Nb-He	Present value	Reference values
Tetra.	3.46	$3.16^{27}, 3.34^{30}, 3.41^{31,24}, 3.45^{16}, 3.46^{18}$	Tetra.	3.18	$3.05^{27}, 3.13^{18}$
Octa.	3.59	$3.42^{27}, 3.60^{16}, 3.65^{30}, 3.68^{24}, 3.74^{31}, 3.79^{18}$	Octa.	3.34	$3.26^{27}, 3.40^{18}$
E_{binding}	1.79	$1.62^{\boxed{31}}, 1.67^{\boxed{32}}, 1.79^{\boxed{18}}, 1.81^{\boxed{16}}$	E_{binding}	1.49	$1.49^{\boxed{18}}.1.67^{\boxed{27}}$
$E_{\rm mig}$	0.09	$0.09^{30,18}, 0.10^{32}, 0.11^{16}$	$E_{\rm mig}$	0.11	$0.09^{\boxed{18}}$
V-He	Present value	Reference values	OCCUPATION AND ADDRESS OF THE PARTY OF THE P		
Tetra.	3.20	$2.94^{27}, 3.09^{24}, 3.17^{18}$			
Octa.	3.35	$3.17^{27}, 3.31^{24}, 3.40^{18}$			
E_{binding}	1.16	$0.91^{27}_{-}, 1.16^{18}_{-}$			
$E_{\rm mig}$	0.11	0.09 18			

- We have developed the interatomic potential to describe the interaction of He atoms with all atoms in HEA composition. The interactions are purely repulsive, the HEA is described by previously developed tabGAP potential
 - [J. Byggmästar, K. Nordlund, and F. Djurabekova, Simple machine-learned interatomic potentials for complex alloys, Phys, Rev. Materials 6 (8),2022.]
- Tabel 2 illustrates the comparison of formation, migration and binding energies for He atoms in monoelemental metals.



Binding energy

 $E_{\text{binding}}(D_1, D_2) = E(D_1) + E(D_2) - E(D_1 + D_2) - E_{ref}$

Pure metals



References for the DFT values:

Ta: You et al, Jour. of Nucl. Mat., 2018(499).

W: Becquart et al, Jour. of Nucl.

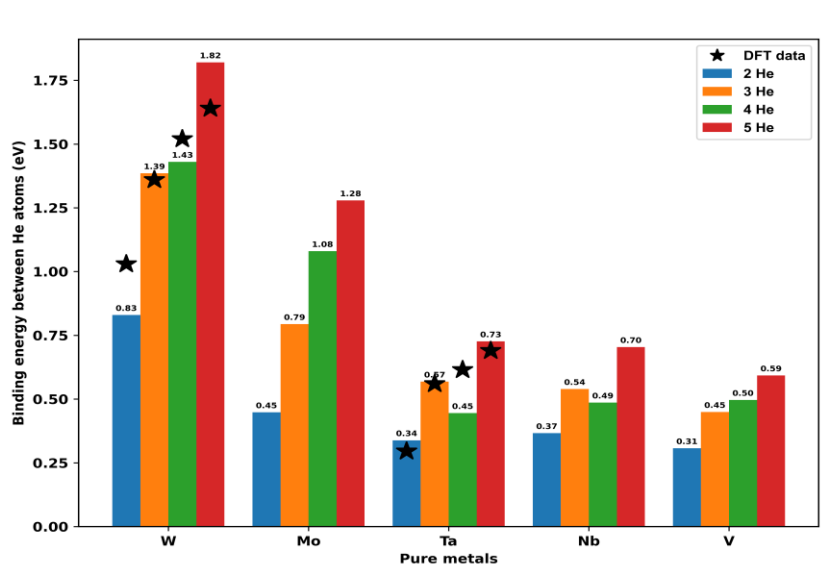
Mat., 2009(385).

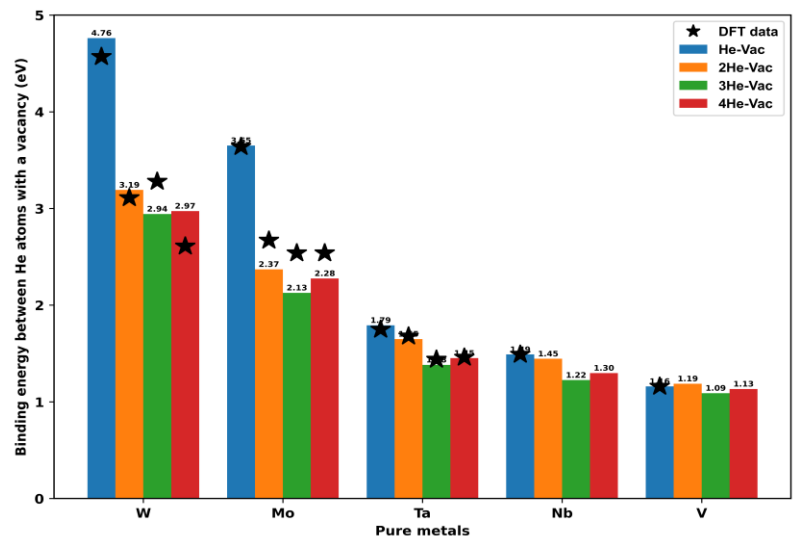
W: Becquart et al, Jour. of Nucl. Mat., 2009(385).

Mo: Runnevall et al, Jour. of Phys.: Cond. Mat., 2009(21).

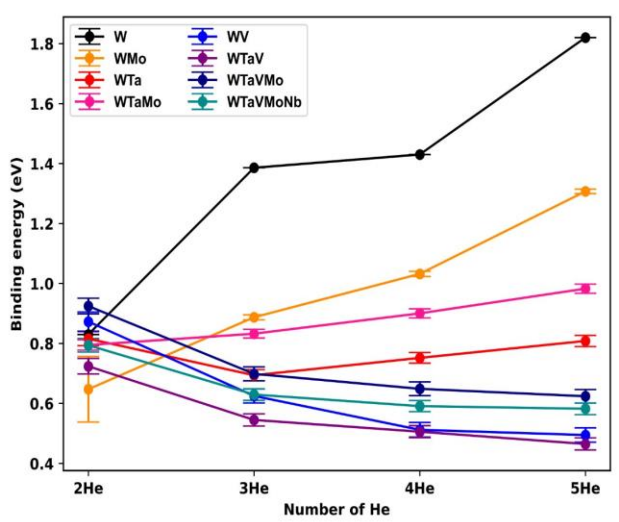
Ta: Omori et al, Nucl. Mat. and Ener., 2018(16).

Nb & V: Jiang et al, Phys. Chem. Chem. Phys., 2018(25).

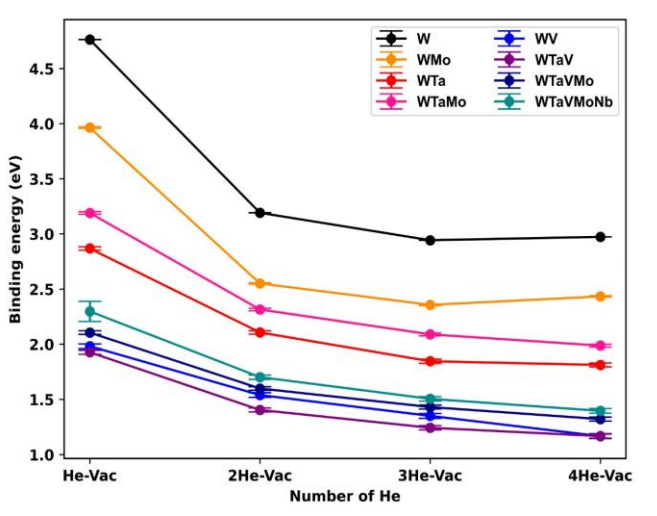




W and W-based alloys



He-He



He-Vac

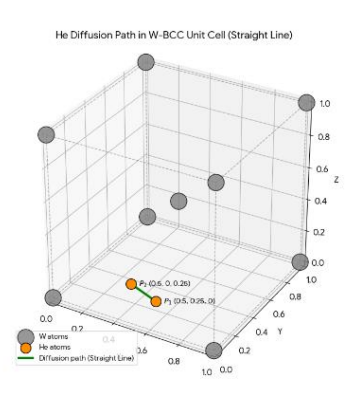


Average migration energy of a He atom



(calculated by NEB)

He position	WMo	WTa	WTaMo	WV	WTaV	WTaVMo	WTaVMoNb
(0.5,0.25,0)*a (0.5,0,0.25)*a (a: lattice constant)	0.2576± 0.0034	0.3021± 0.0056	0.3234± 0.0040	0.6313± 0.0095	0.5300± 0.0068	0.5152± 0.0060	0.4584± 0.0049

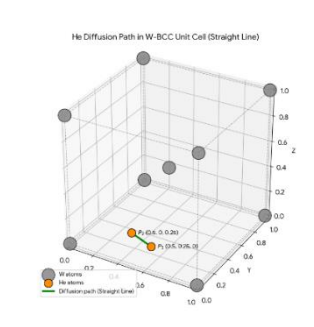


Migration path

Pure metals

Migration energy	Мо	Nb	Ta	V	W
DFT data[1]	0.07	0.11	0.09	0.11	0.12
Our results	0.06	0.09	0.09	0.09	0.06

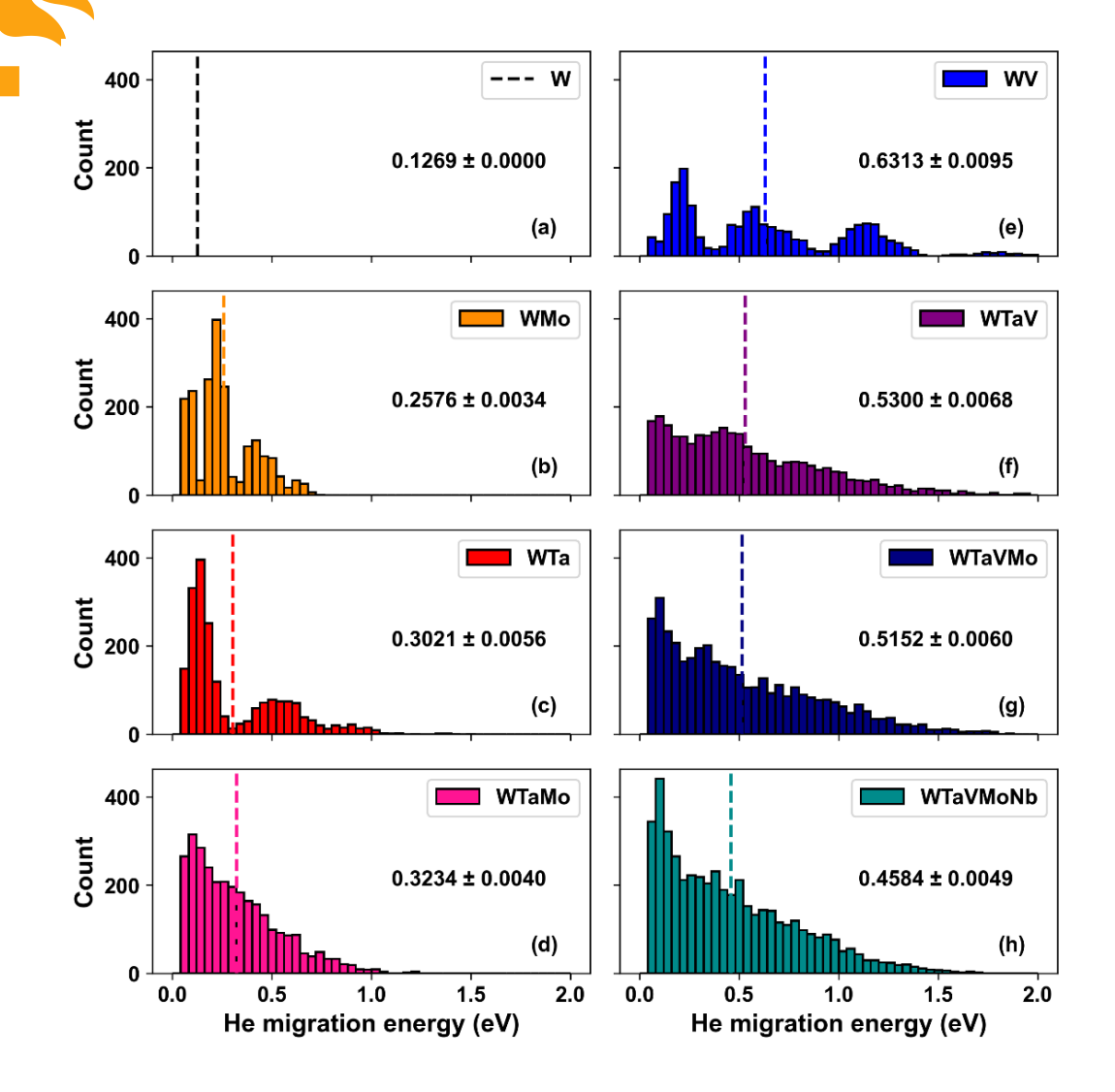
Migration energy of a He atom



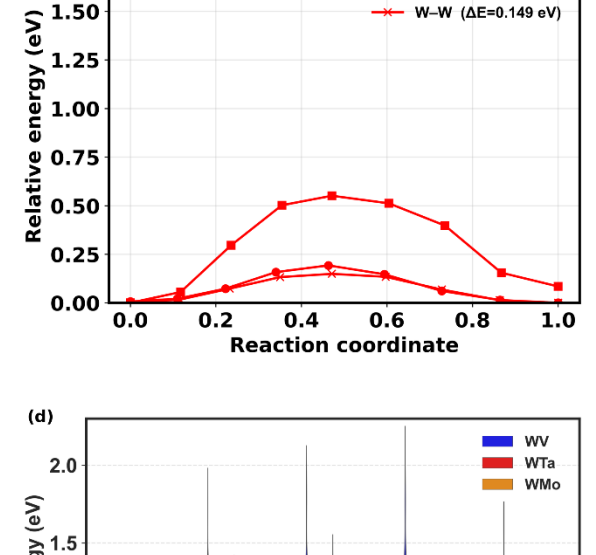


W-Ta (ΔE=0.551 eV)

Ta-Ta (ΔE=0.192 eV)



--- W-V (ΔE=1.806 eV) WTa -- V-V (ΔE=0.164 eV) 1.50 (o. 1.25) 1.25 1.00 (Ne) 1.25 1.00 W-W (ΔE=0.283 eV) Relative 0.50 Relative 0.50 0.25 0.25 0.00 0.00 0.0 0.2 0.6 8.0 1.0 **Reaction coordinate**



1.75 WMo W-Mo (ΔΕ=0.474 eV)
1.50 Mo-Mo (ΔΕ=0.231 eV)
1.25 Mo-Mo (ΔΕ=0.231 eV)
1.25 Mo-Mo (ΔΕ=0.231 eV)
2.0 Mo-Mo (ΔΕ=0.231 eV)
1.00 Mo-Mo (ΔΕ=0.231 eV)
1.00 Mo-Mo (ΔΕ=0.231 eV)
2.0 Mo-Mo (ΔΕ=0.474 eV)
2.0 Mo (ΔΕ=0.474

2.0 WTa WMo WMo O.5 0.20 21 -40 41 - 60 61 - 80 81 - 100 W concentration (%)

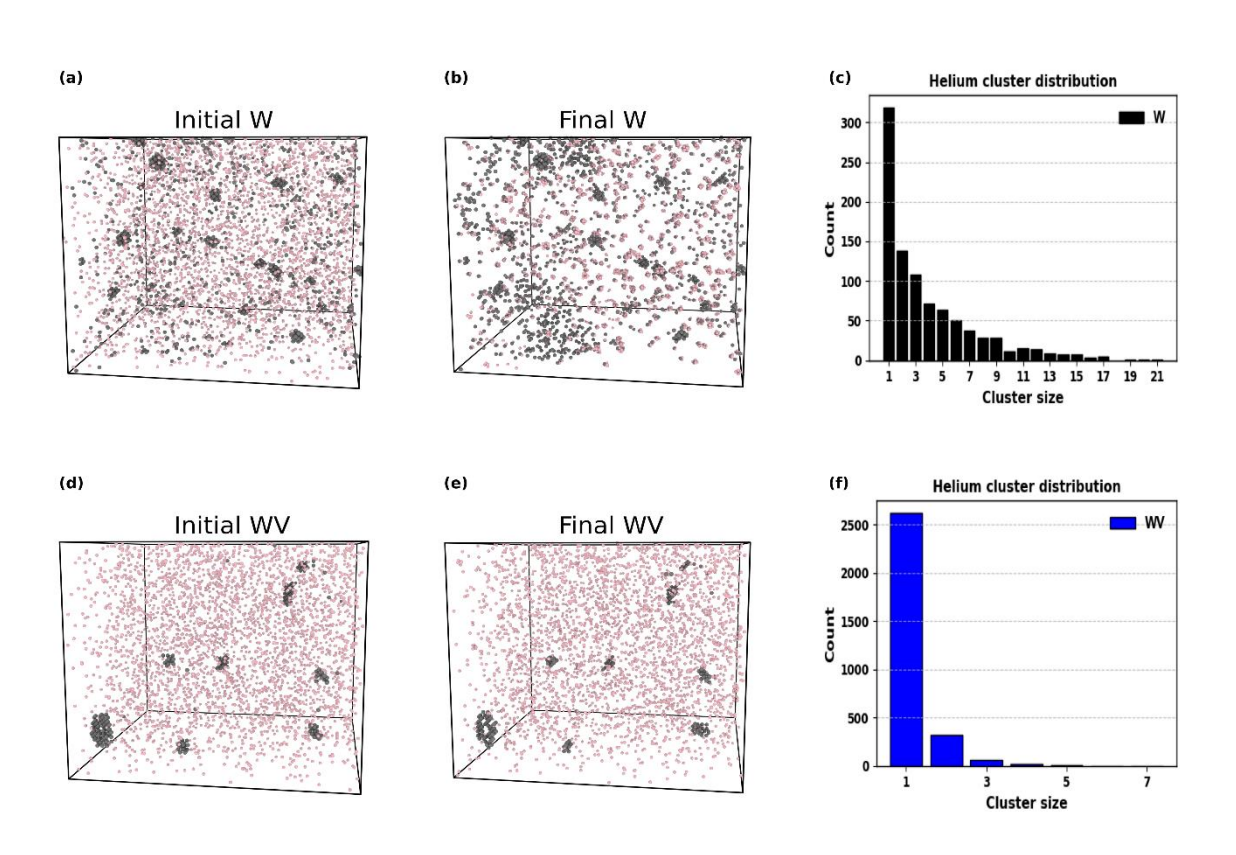
The distribution of migration energies

Effect of W concentration in the environment on the migration of He atoms 11

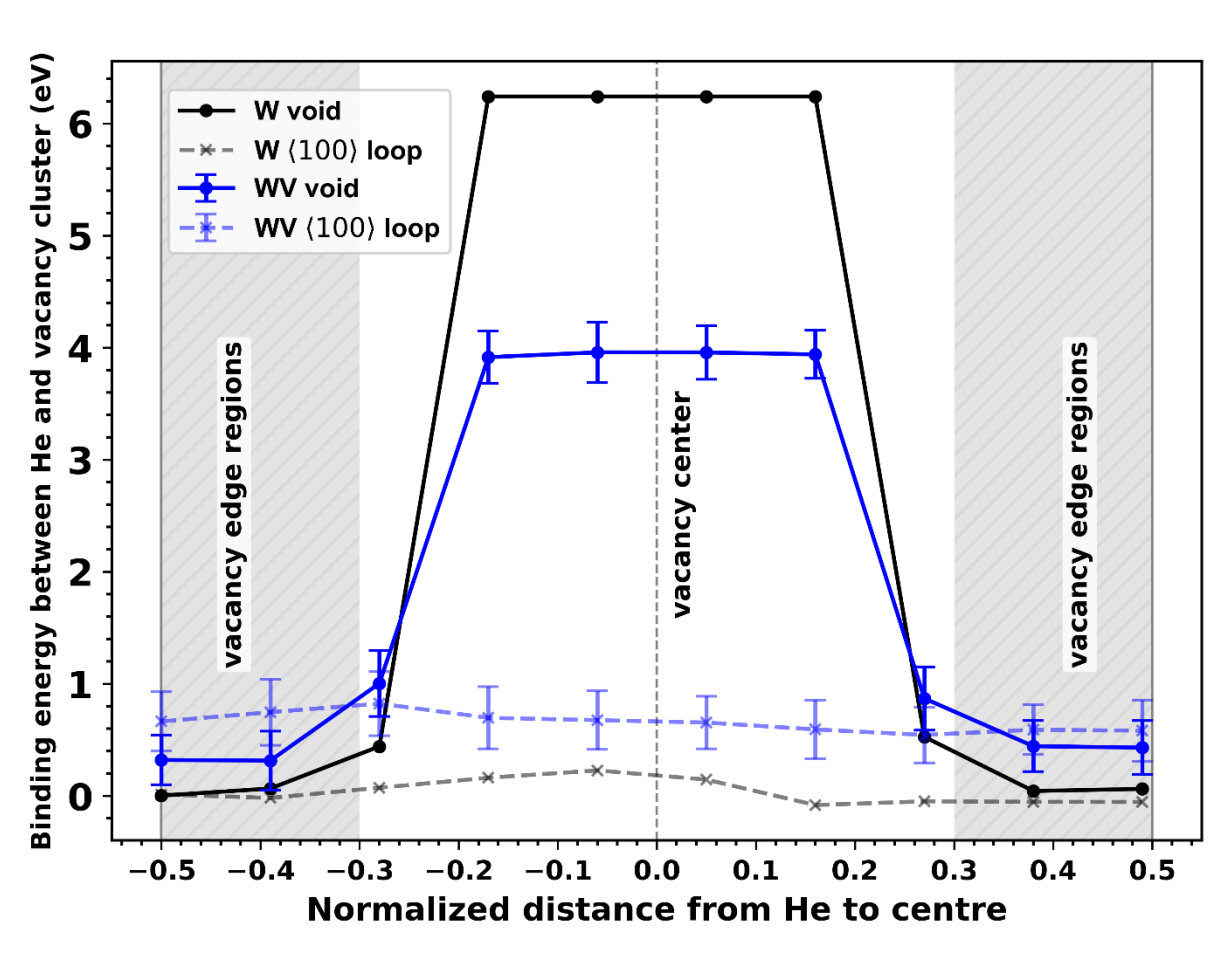


Cascade simulations with He implantation





Snapshots of He atoms in systems of 0.3 dpa radiation damage, showing vacancies (gray atoms) and He (pink atoms).



Binding energy of a single He atom with a void (100vacancies) and a $\langle 1 \ 0 \ 0 \rangle$ vacancy loop (101 vacancies) in W and WV.



WP3(exp) "He irradiation of REAA in three energy regimes (low, medium and high) at fusion reactor relevant temperatures. In-situ and ex-situ characterization of He bubble growth in REAA of different compositions"







- We have prepared two types of samples:
 - 1. Bulk samples (Sample preparation: cutting, polishing)
 - from VTT (Arc Melting binary alloys, WMo, WTa, WV, + pure W)
 - from IPFN (Institute for Plasma Research and Nuclear Fusion, Portugal)
 - 2. Thin layers (Magnetron sputter deposition, WV binary alloys, 50-100nm on MgO substrates)
 - University of Helsinki
- Two ways to insert ³He into the samples:
 - 1. ³He plasma exposure (low energy 300 eV, medium flux 10¹⁴ cm⁻².s⁻¹
 - 2. ³He implantation (Pelletron accelerator) 0.5 MeV, low flux 7x10¹⁰ cm⁻².s⁻¹
- Characterization techniques:
 - Nuclear reaction Analysis (NRA): Detection of ³**He** with a deuteron beam (900 keV) using ²H (³He, ⁴He)¹H reaction
 - Rutherford Backscattering (RBS)
 - Scanning Electron Microscopy Electron Dispersive spectroscopy (SEM-EDS)
 - Atomic Force Microscopy (AFM)

³He plasma exposure in thin layers + bulk samples

Masked

³He plasma exposure in thin layers in PIMAT:





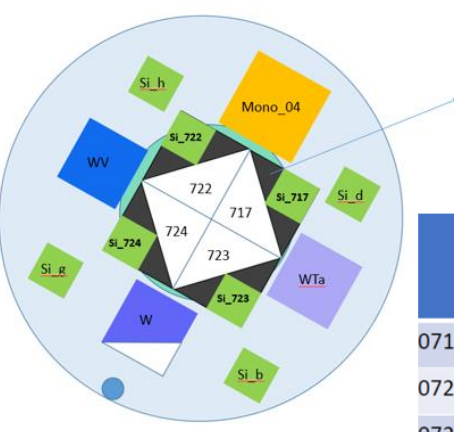
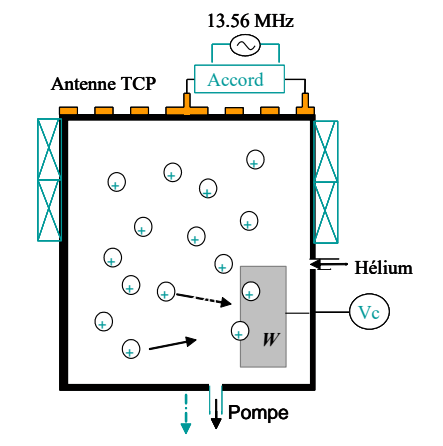
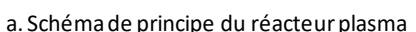
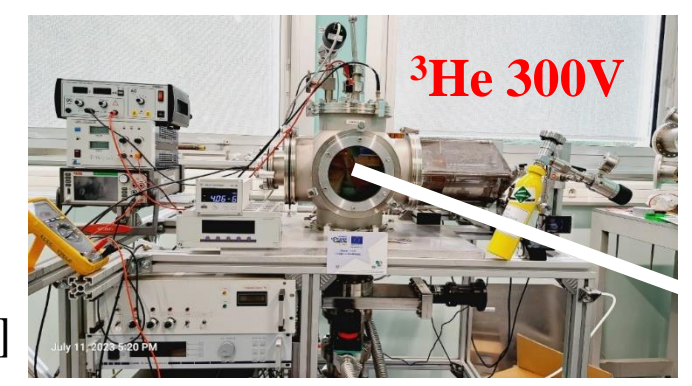
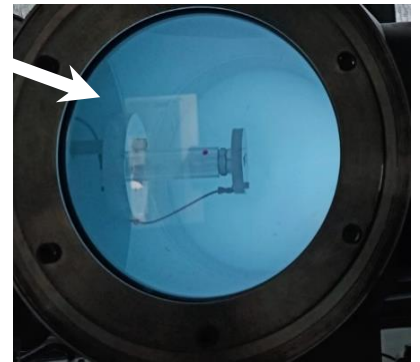


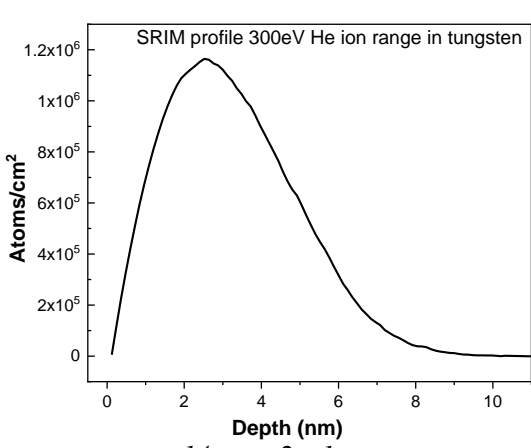
Table 1: Exposed thin-layer samples Thickness Temperature (C) Surface Oxygen estimate(nm) estimate(%) Measured at 09/05/2025 0717 W 300 ~ 4% 150-200 0722 W+C 300 100-150 0 0723 WV+C 300 50-100 ~3% 0724 WV 50-100 ~10% 300











Flux 1,5x10¹⁴ cm⁻²s⁻¹ Fluence estimated at 8x10¹⁶ cm⁻²



He release in DIADDHEM



• He release as a function of temperature () in W bulk alloys and thin layers exposed to ³He in PIMAT:

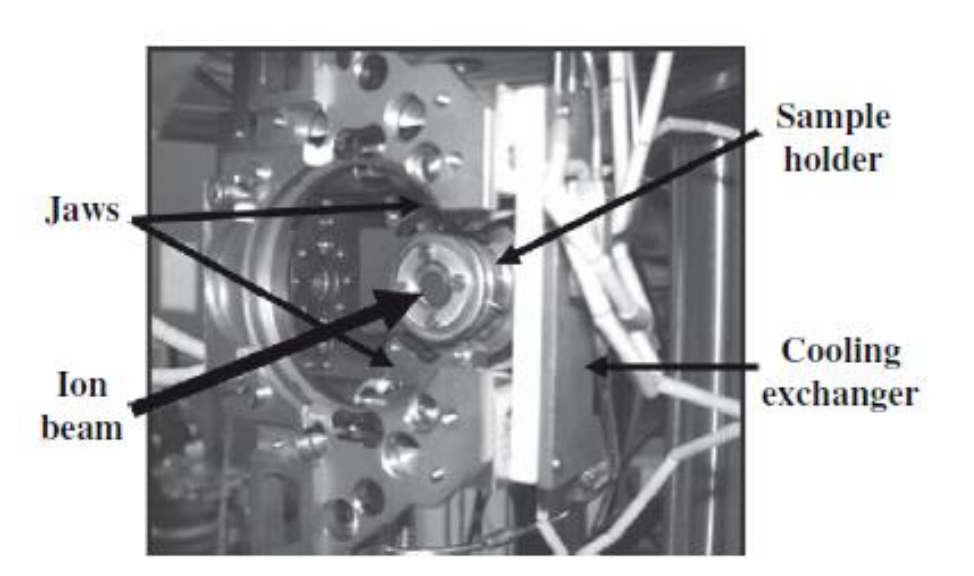
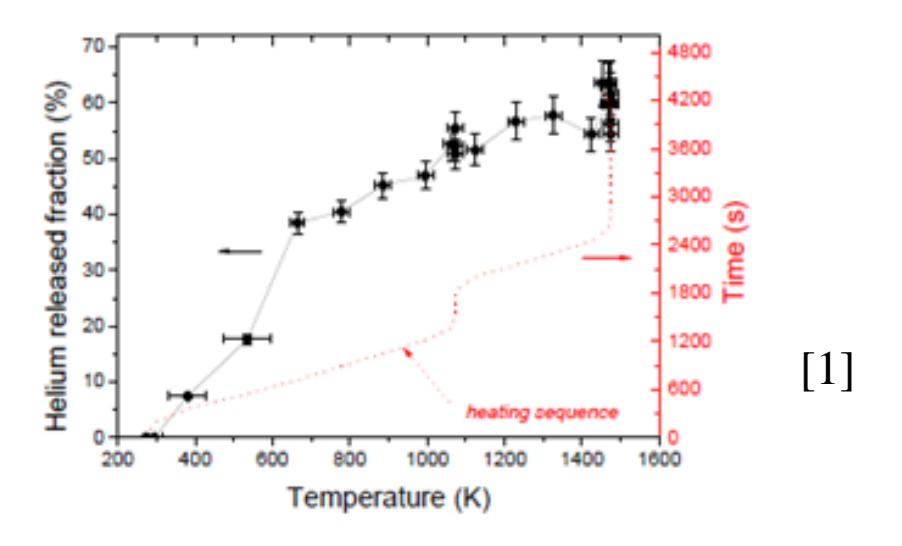


Fig. 1. Photography of the DIADDHEM core.

DIADDHEM - Device for Analyzing the Diffusion of Deuterium and Helium in Materials

	Sample (MgO substrate)	Temperature (C)	Thickness estimate(nm)	Surface Oxygen estimate(%) Measured at 09/05/2025	Holes	Grain sizes
0717	W	300	150-200	~ 4%	No	Same as 0718
0722	W+C	300	100-150	0	No	Same as 0718
0723	WV+C	300	50-100	~3%	No	Single crystal
0724	WV	300	50-100	~10%	No	Single crystal

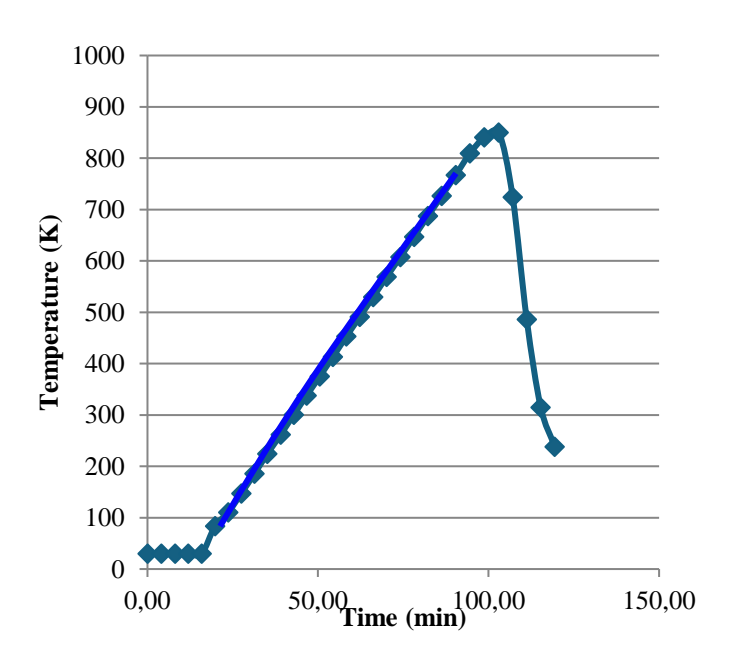




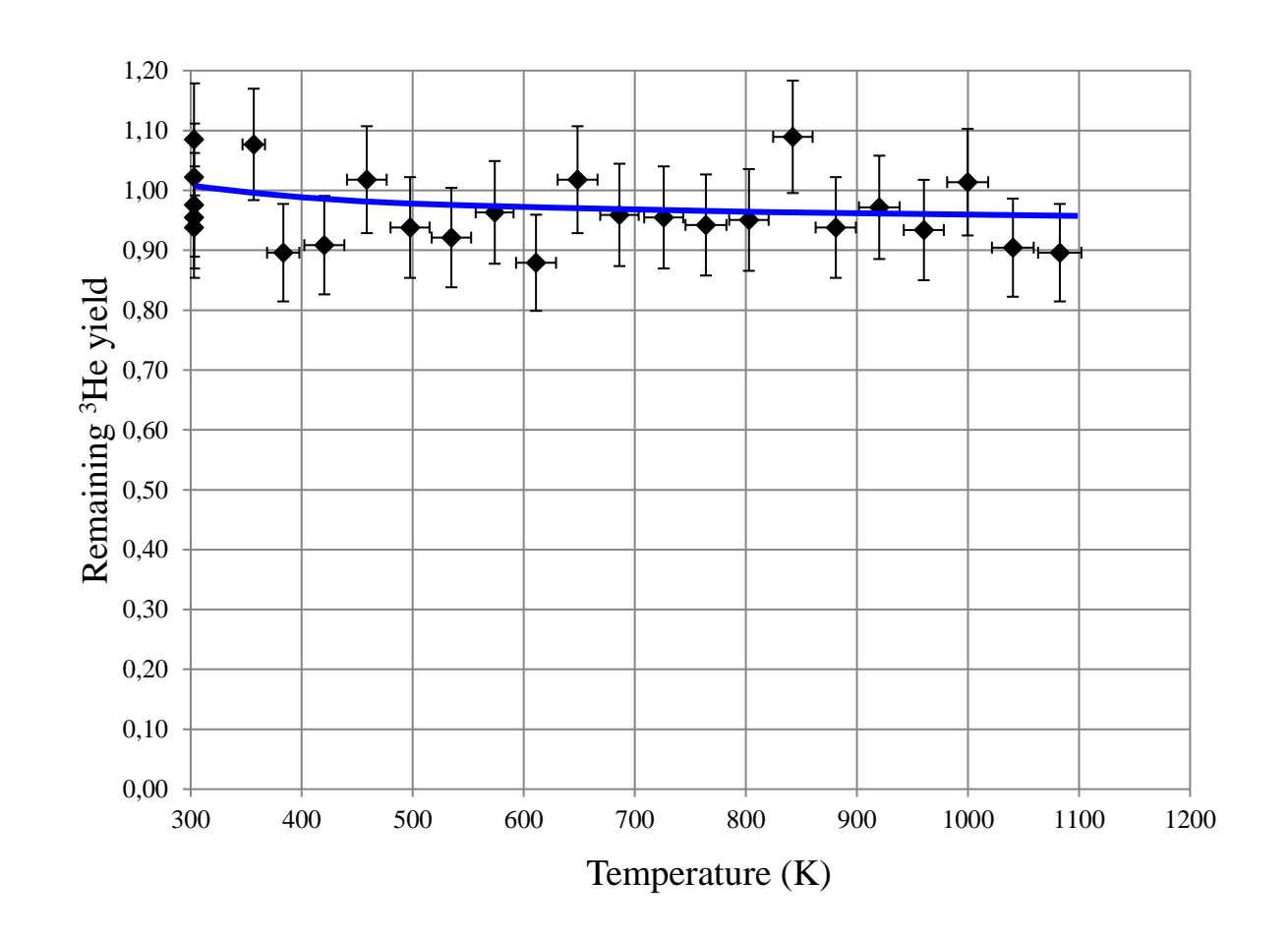
In situ release in DIADDHEM



• W single crystal (W-M-M-04)



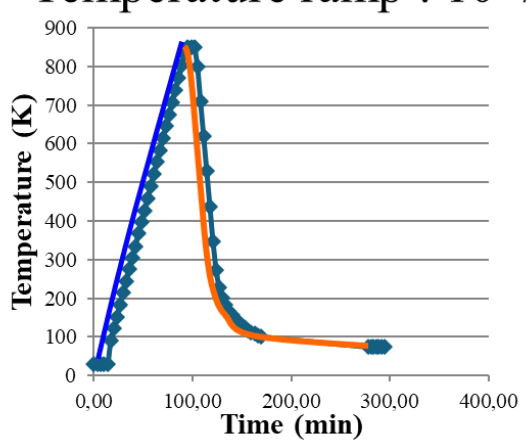
Temperature ramp: 10°/min



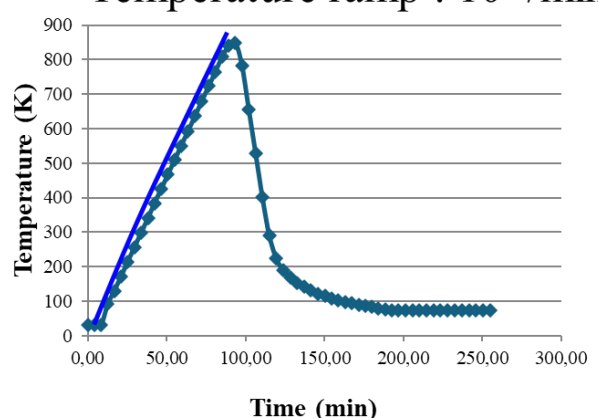
In situ release in DIADDHEM

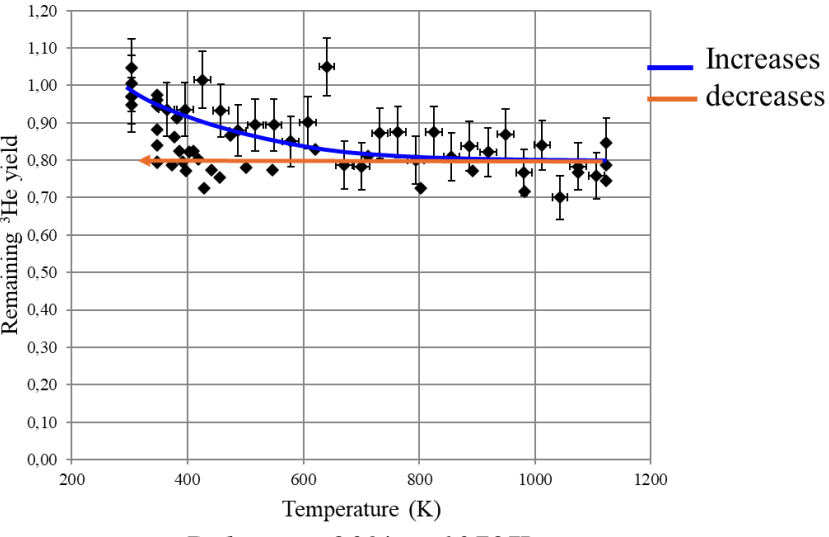


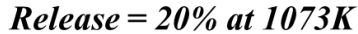
- WV/MgO (0724, W₅₀V₅₀)
 - Temperature ramp: 10°/min

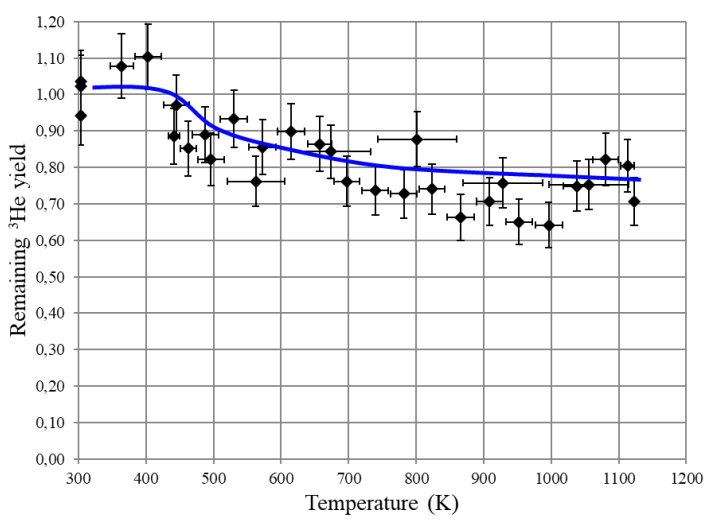


- WV/MgO (723, W₅₁V₄₉+C)
 - Temperature ramp: 10°/min





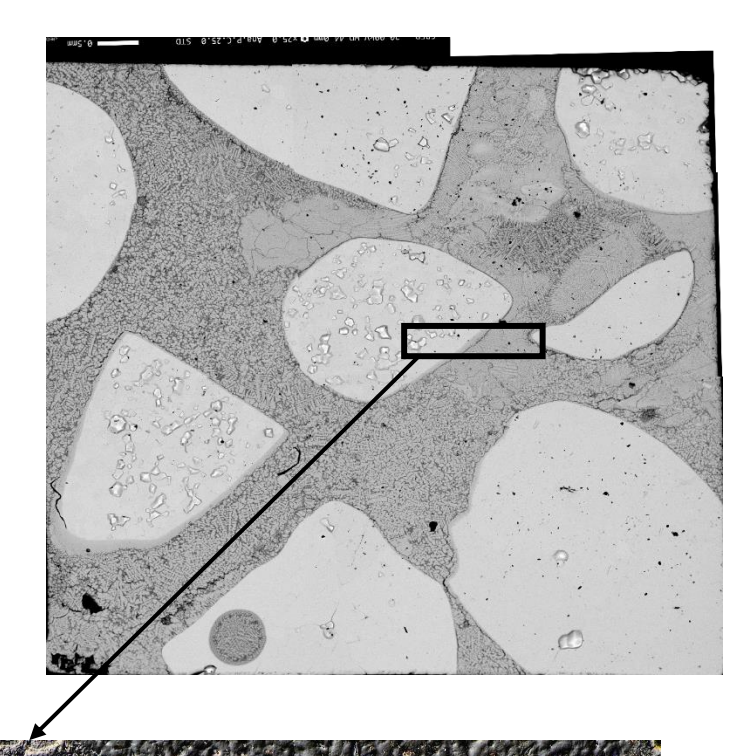


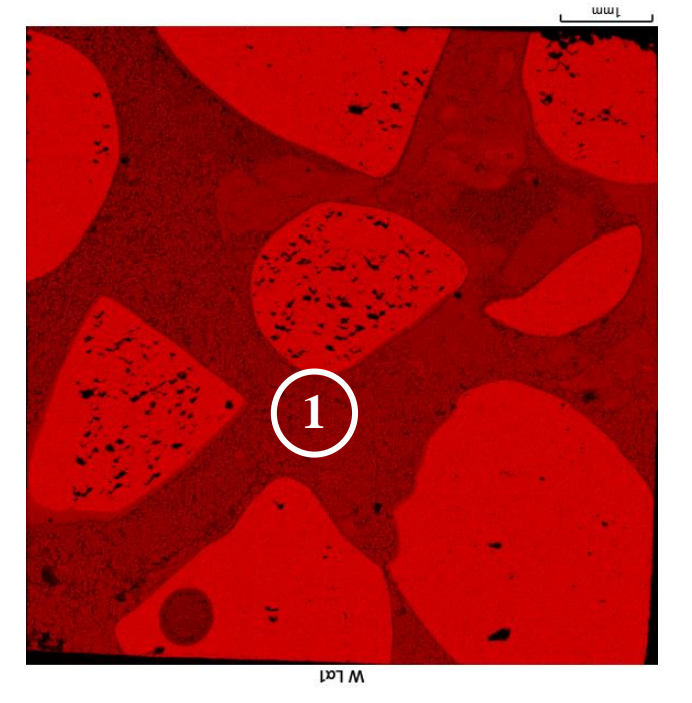


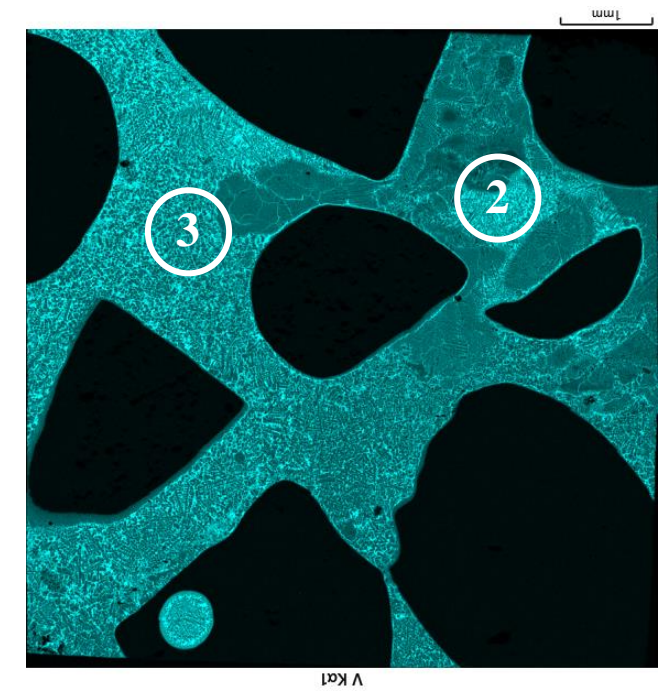




VTT : Evaporation of V during arc melting





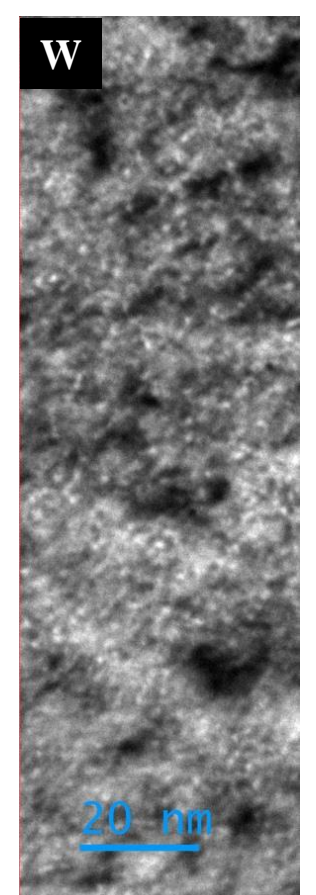


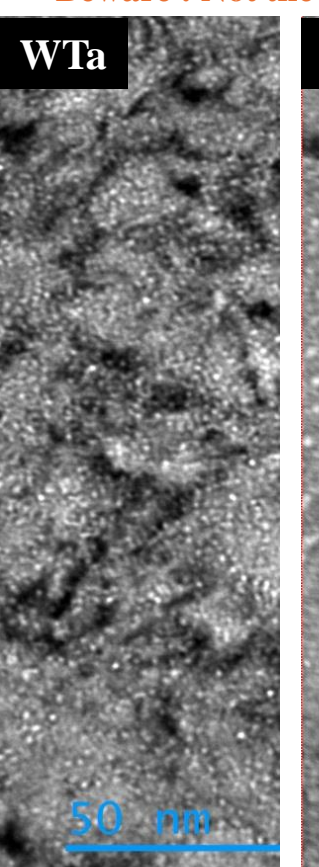
- (1) Zones with pure W and pores
- (2) Zones with heterogeneous concentration of V
- (3) Zones enriched in V

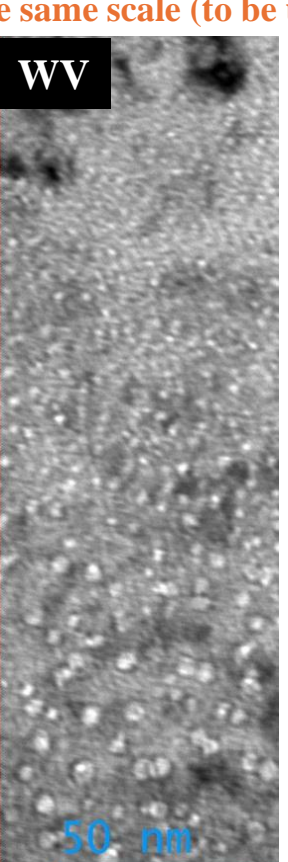


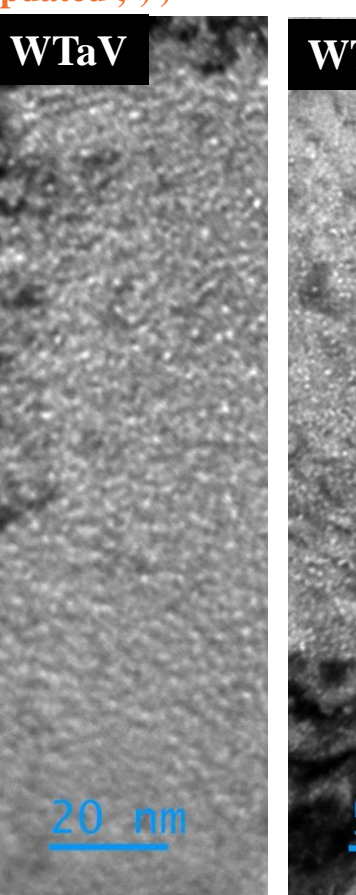
TEM results

Beware! Not the same scale (to be updated ;-))

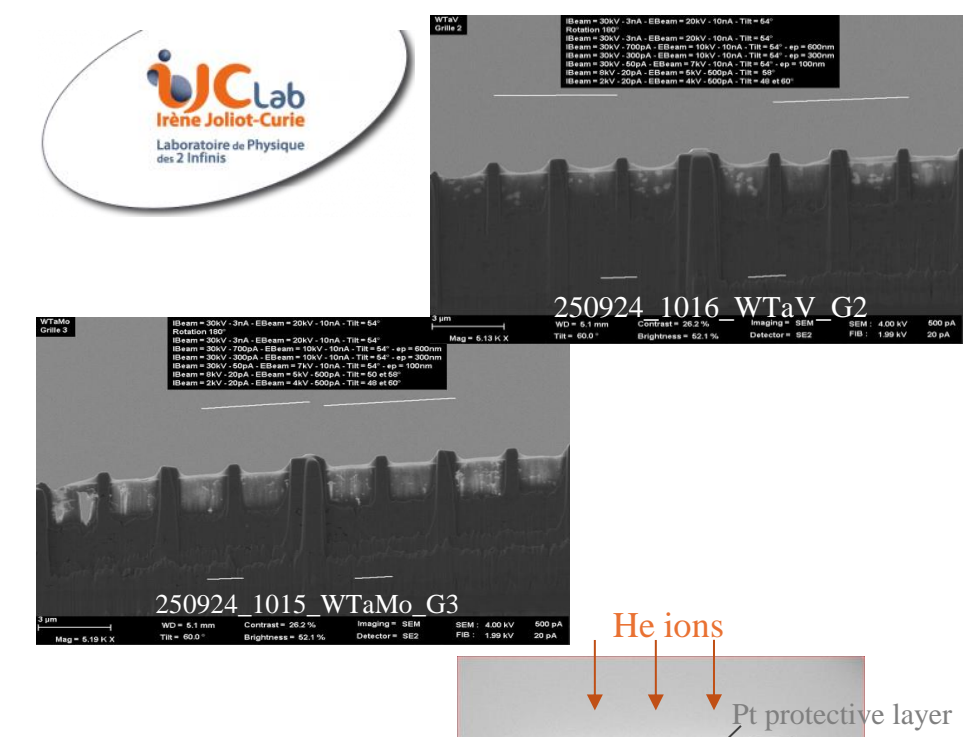












Through focus series of bright field images showing bubbles

See details next slides

Observation if any He bubbles are seen Transmission Electron Microscopy

ex situ (in October/November)

TEM thin foils preparation by FIB

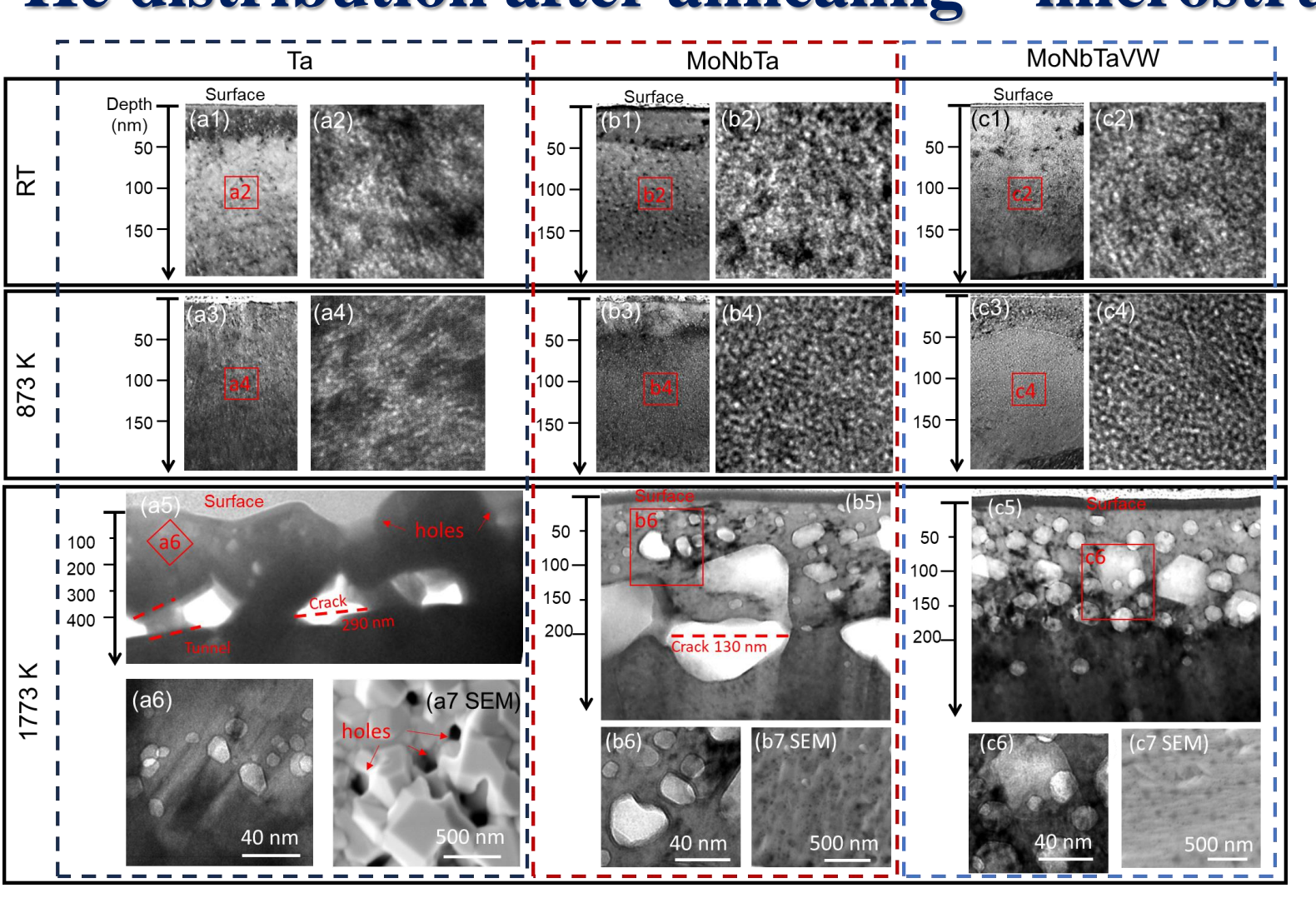
(end Sept./Oct., IEMN and NCBJ)

4C_W_1700X_0091

surface



Alternative BCC HEA with Ta-based composition: He distribution after annealing---microstructure





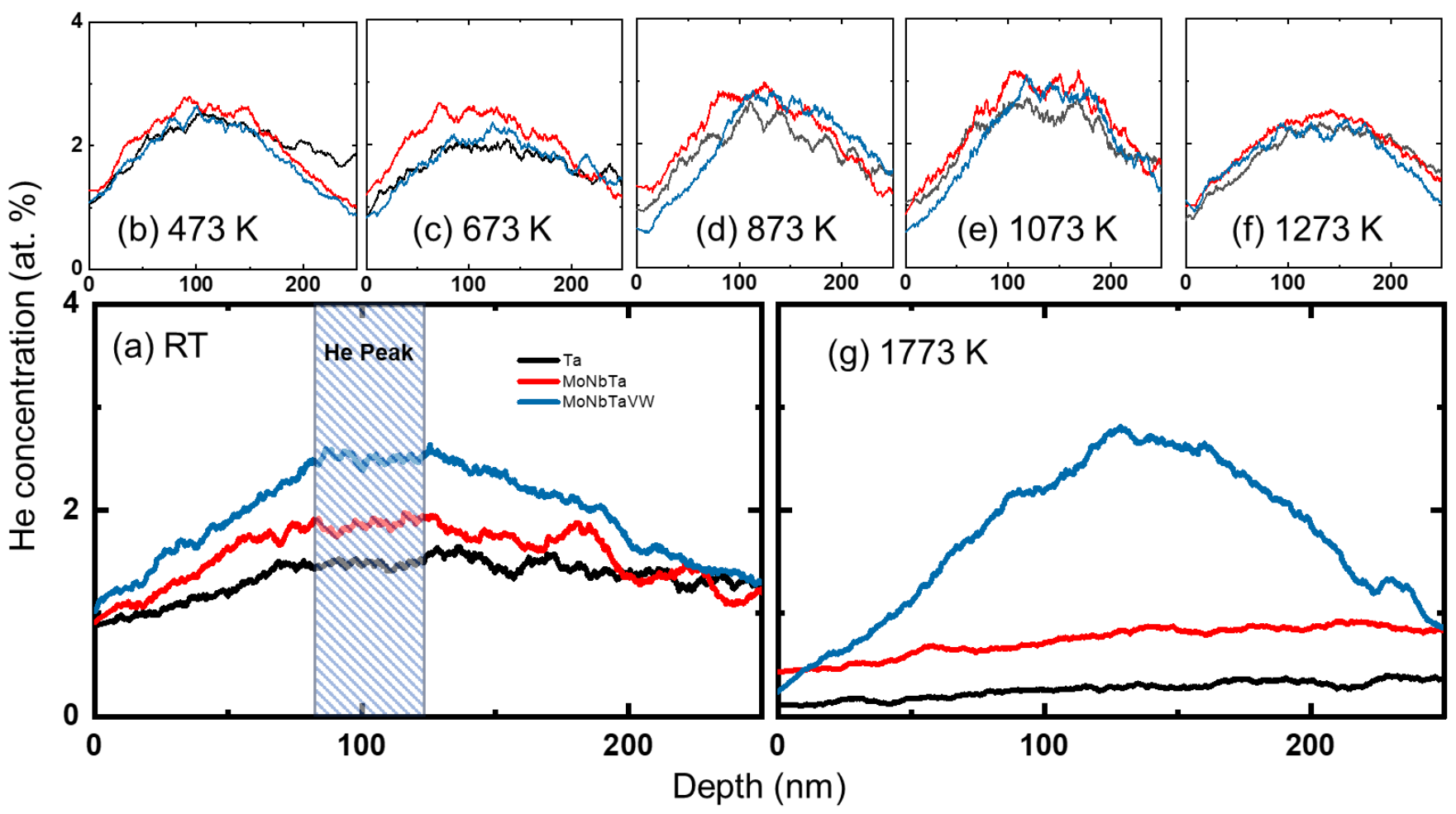
Samples: Arc-melted Ta, MoNbTa, MoNbTaWV, BCC, large grain size (around 100 um),

Irradiation: 5×10^{16} 25 keV He (ions/cm²), at room temperature

- He bubbles are more concentrated at the damage peak in BCC HEA.
- In pure metal Ta, long-range He migration leads to cracks and holes



He depth profile by ERDA



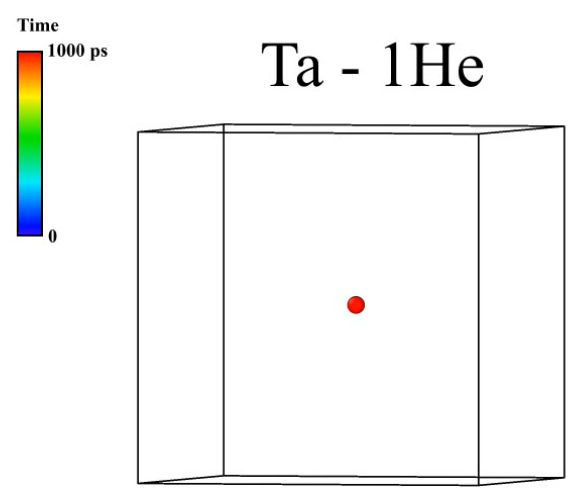


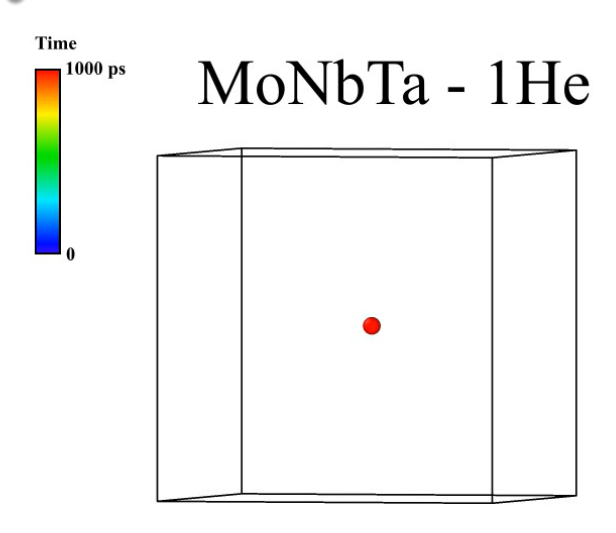
He profiles obtained by ERDA (=Elastic Recoil Detection Analysis) support TEM microstructure results, which suggest that long-range helium migration is limited in BCC HEA

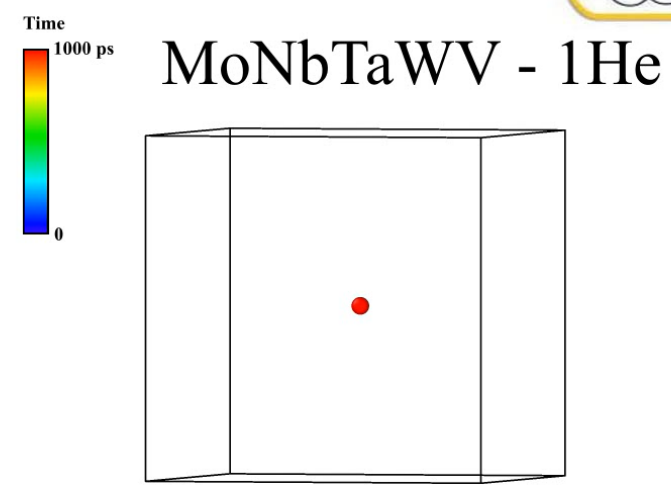


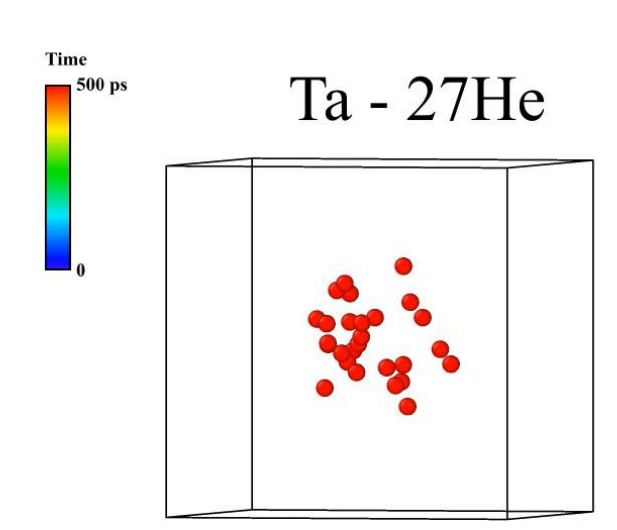
Molecular Dynamics simulation

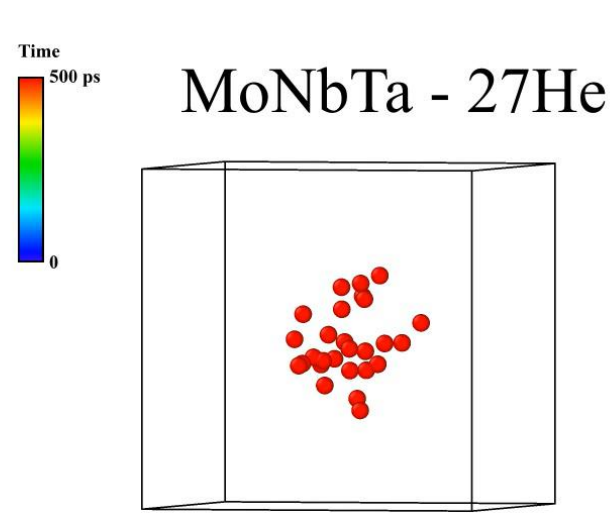


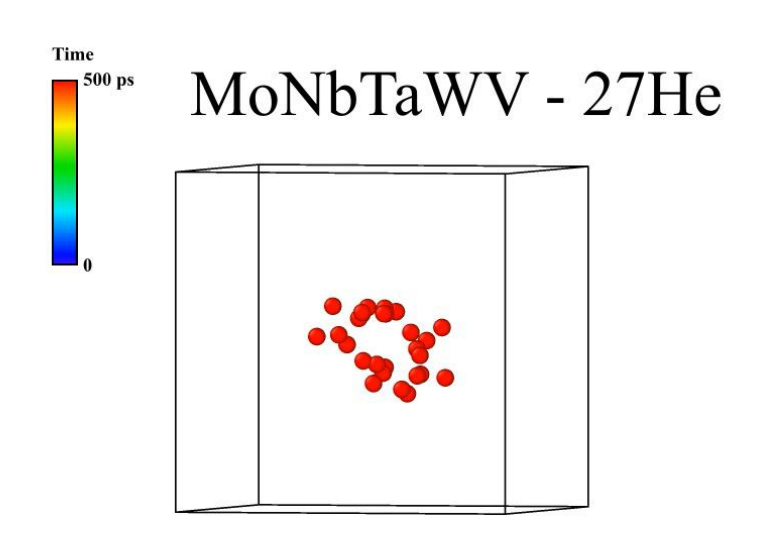






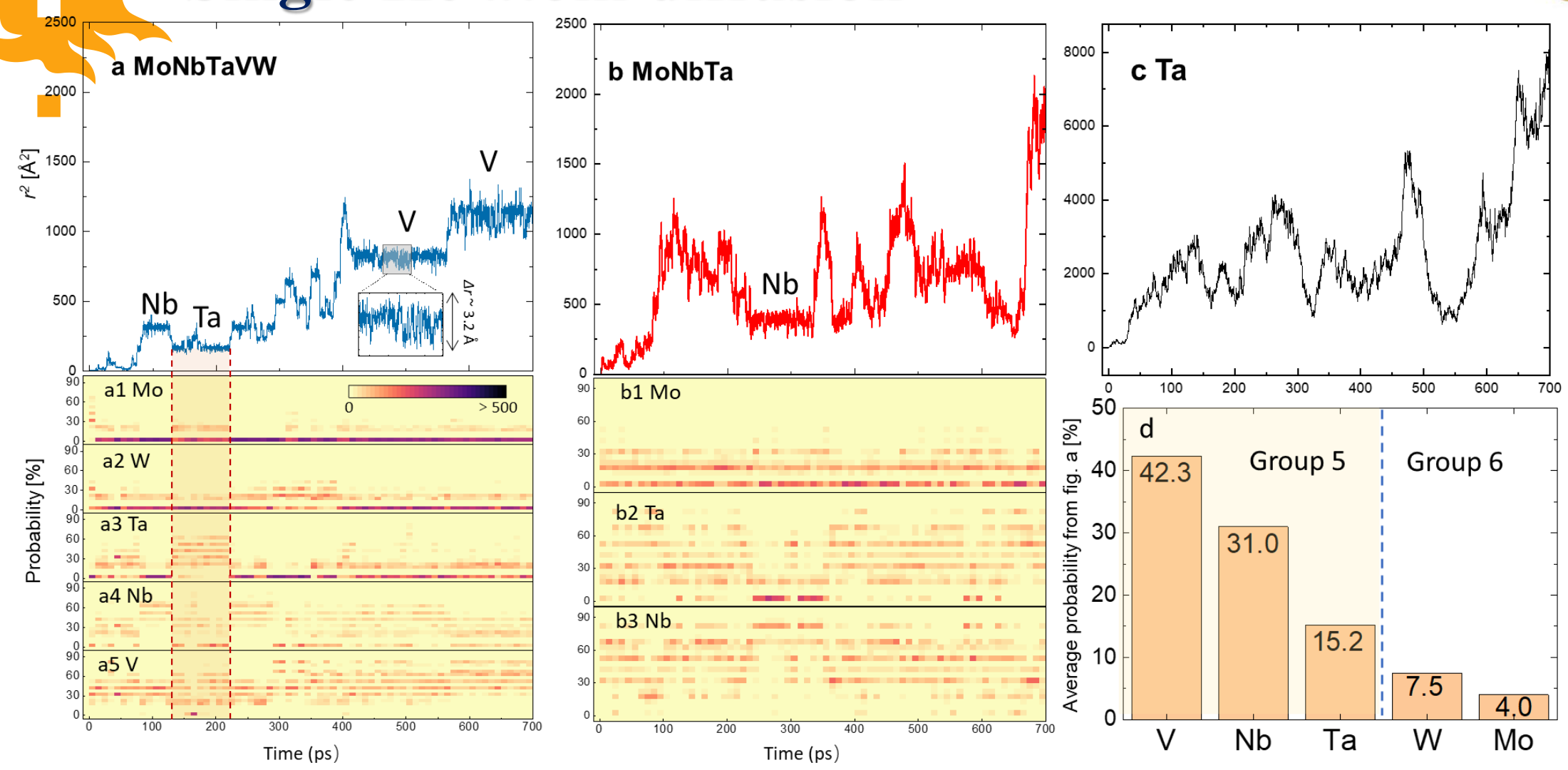






Single He atom diffusion





He tend to trap around Group 5 elements (V, Nb and Ta)



WP4(th) "Simulations of He bubble growth in REAA due to He irradiation with different irradiation energies by means of ML-KMC and ML-MD"

Suppression of He clustering in W across temperature via dilute V alloying AKMC simulation of He-vacancy complex mobility in W and WV



He cluster fraction in WVx and WTax



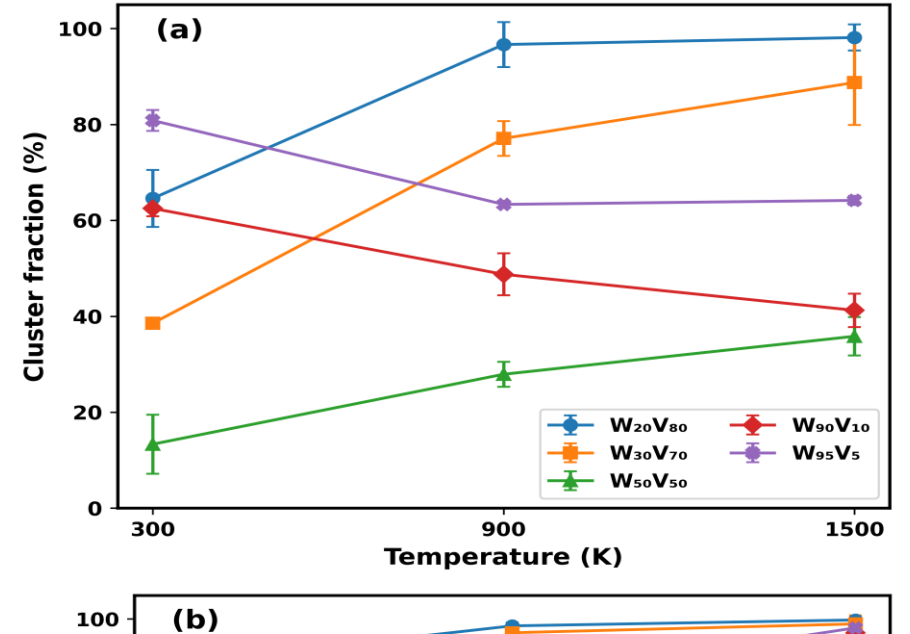
He cluster fraction = 1 - Number of single He atom / Total He number

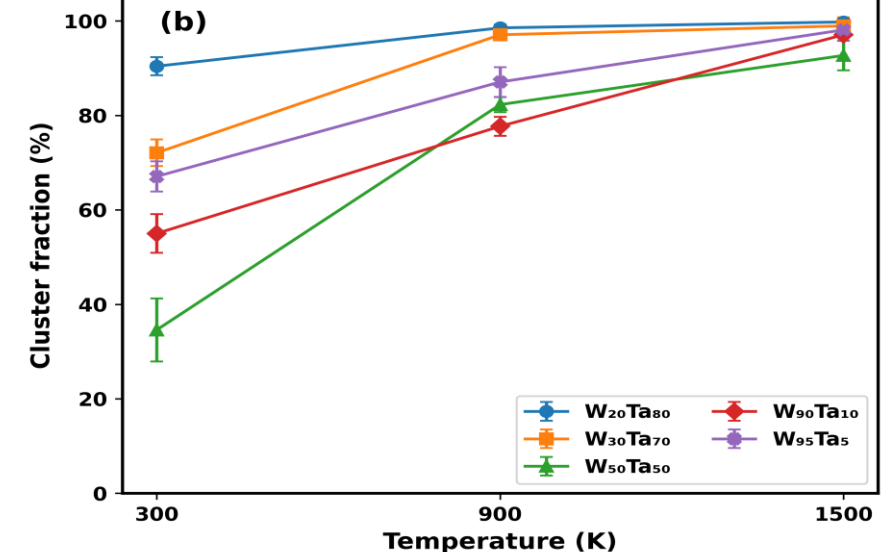
Box size: $20 \times 20 \times 20$ unit cells = 16000 atoms + 1% He (160 atoms)

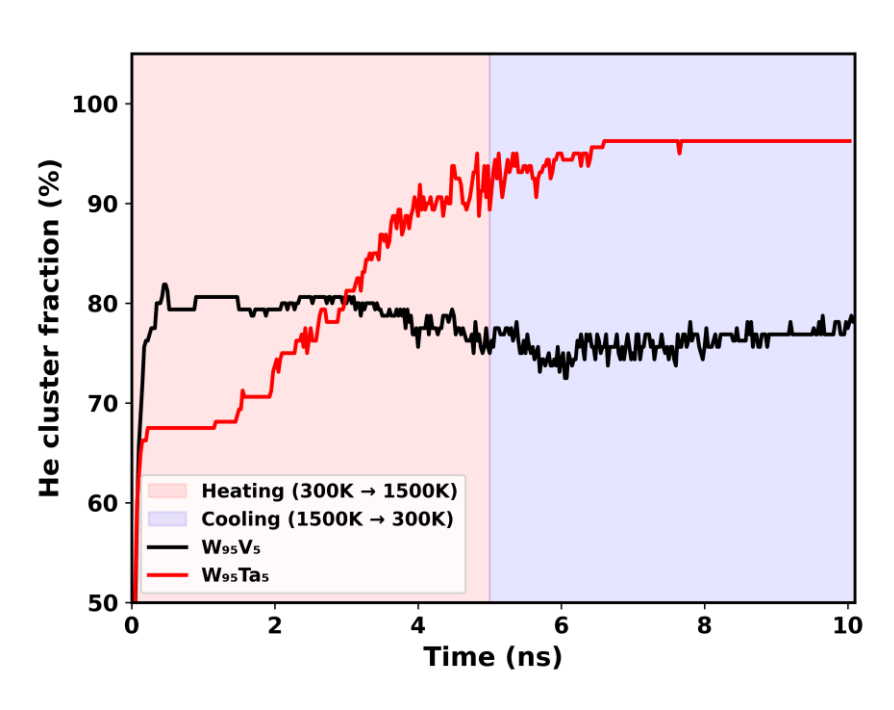
Minimize first

NPT relax 5 ns at 300 K, 900

K and 1500 K





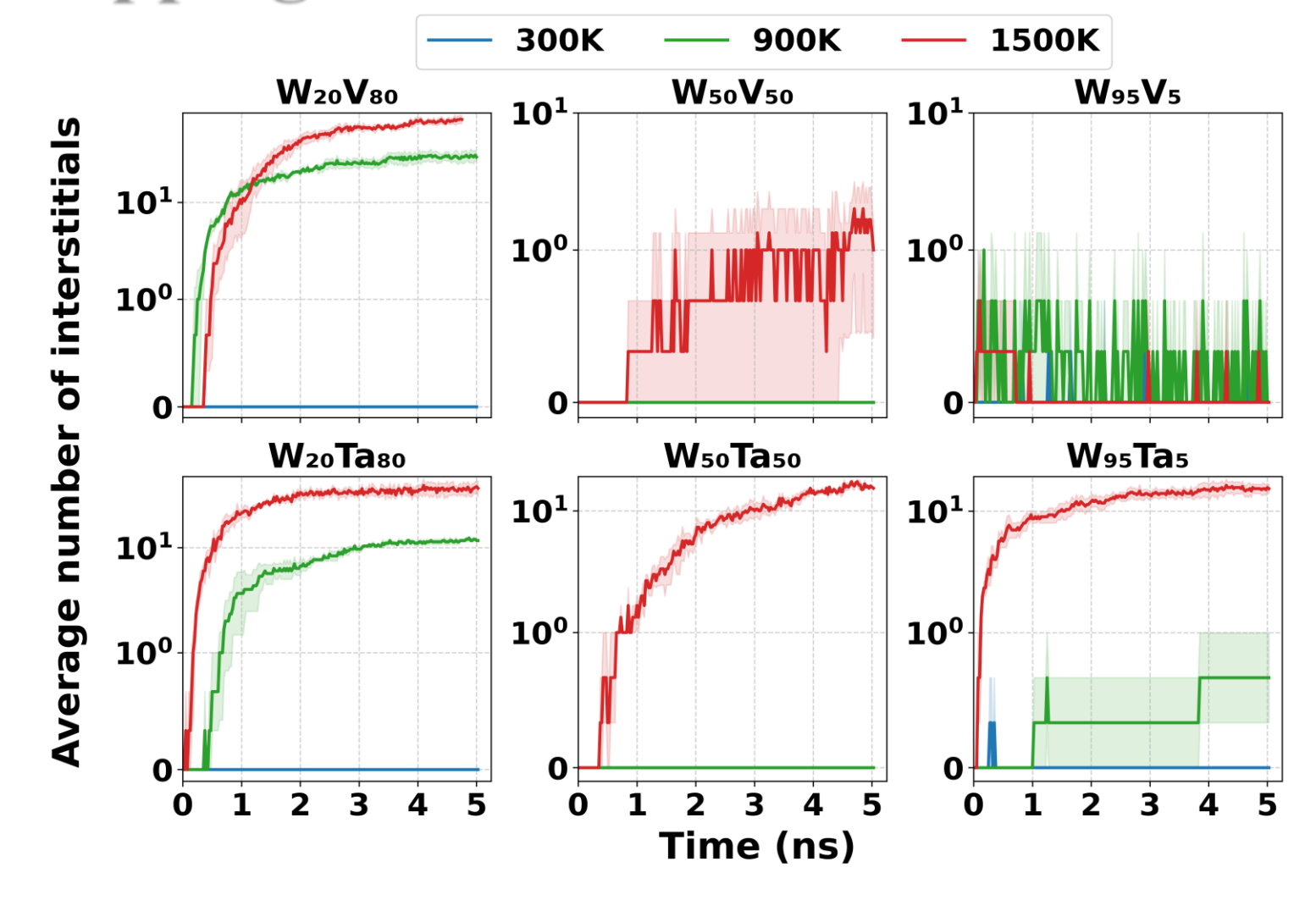


Verification by a thermal cycle.



Self trapping





Evolution of the average number of interstitials in W–V and W–Ta alloys at 300 K, 900 K, and 1500 K without He atoms. (Statistics is given by the three independent runs)

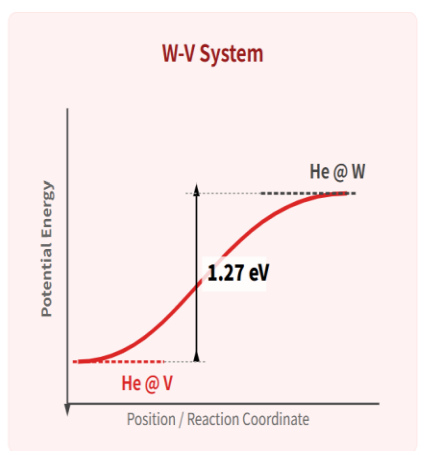


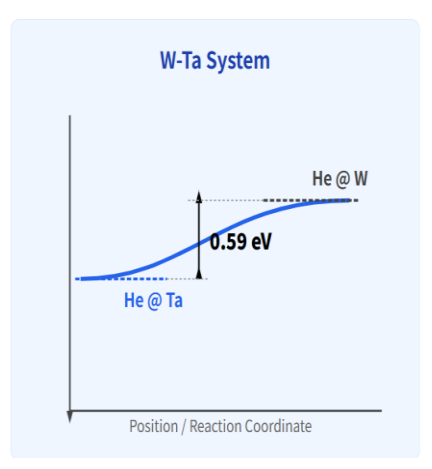
Elements around He



The energy differences were calculated using a 20 * 20 * 20 W supercell with a central solute atom. Values represent the potential energy change when a He atom moves from a bulk-like W environment to a tetrahedral site adjacent to the solute (V/Ta).

Energy Difference between He@Trap and He@W



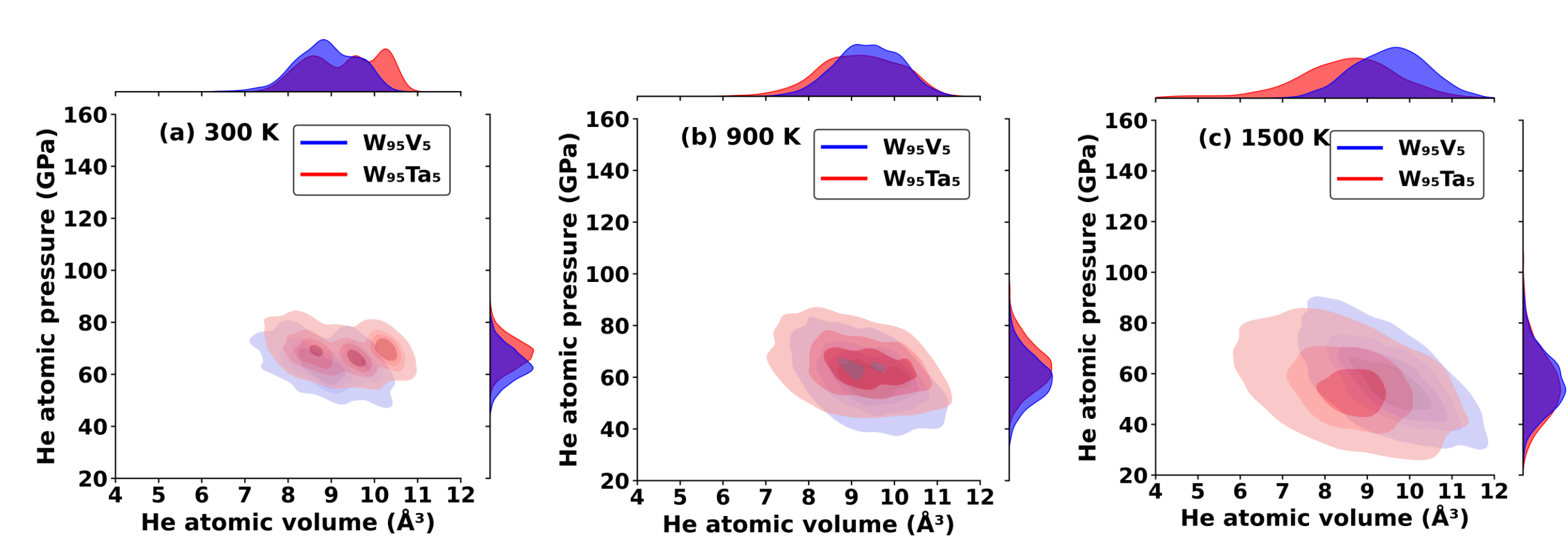


Evolution of the solute concentration around He atoms, in W95V5 and W95Ta5 alloys at 300 K, 900 K, and 1500 K (Statistics is given by 3 independent runs)

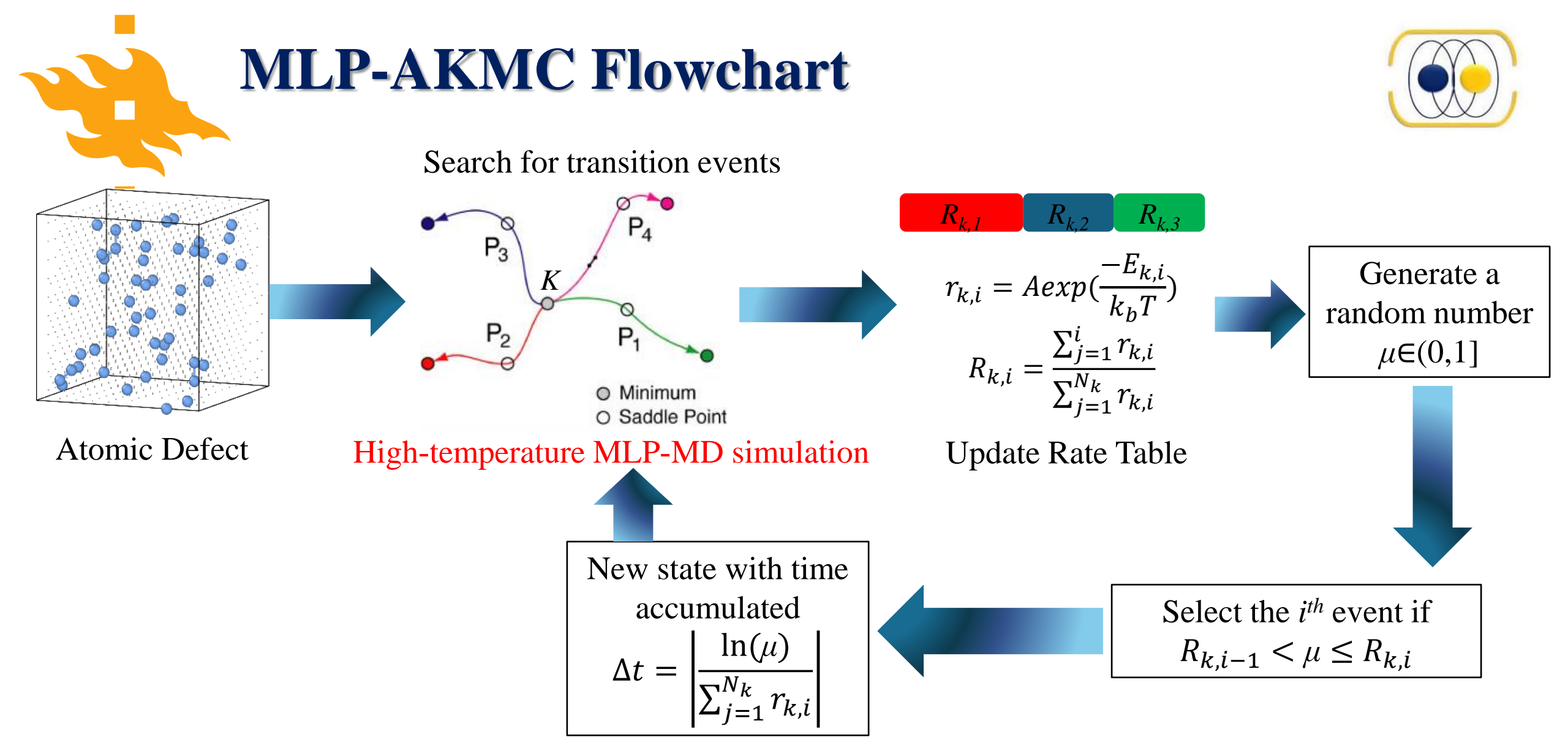


Pressure-volume





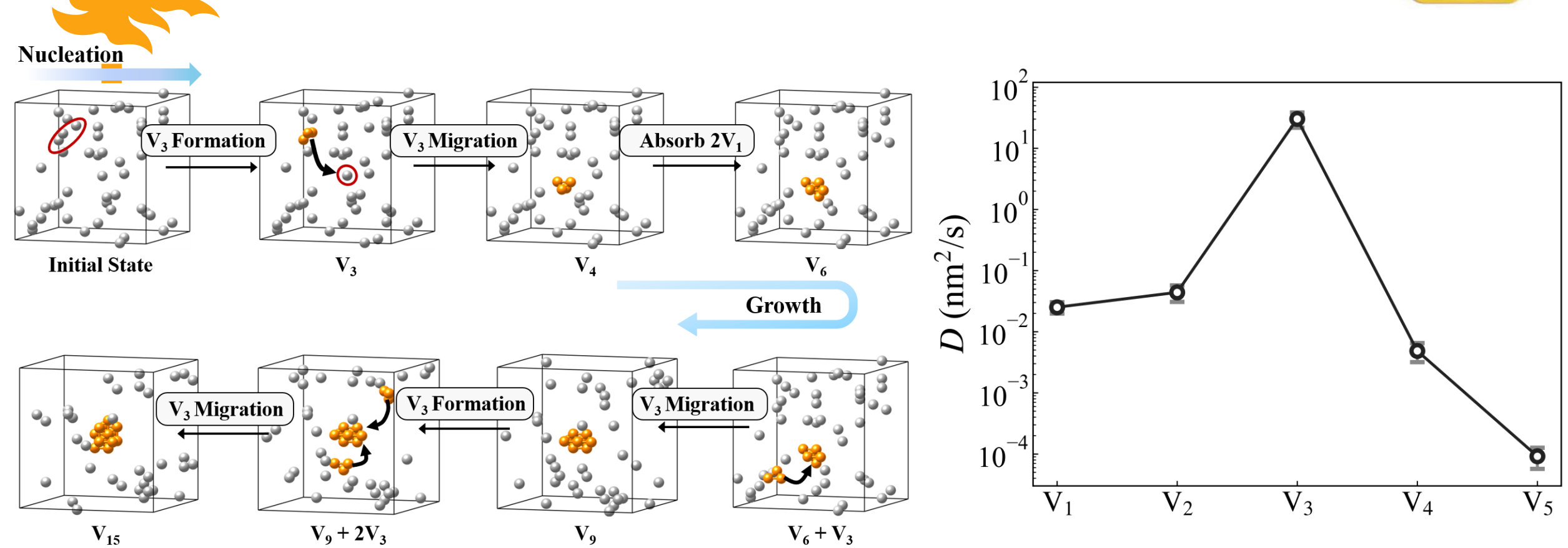
He atomic pressure-volume contour plots and corresponding distributions for W95V5 (blue)and W95Ta5 (red) at (a) 300 K, (b) 900 K, and (c) 1500 K.



To accurately observe the evolution of vacancies on experimental time scales

The importance of V₃ cluster





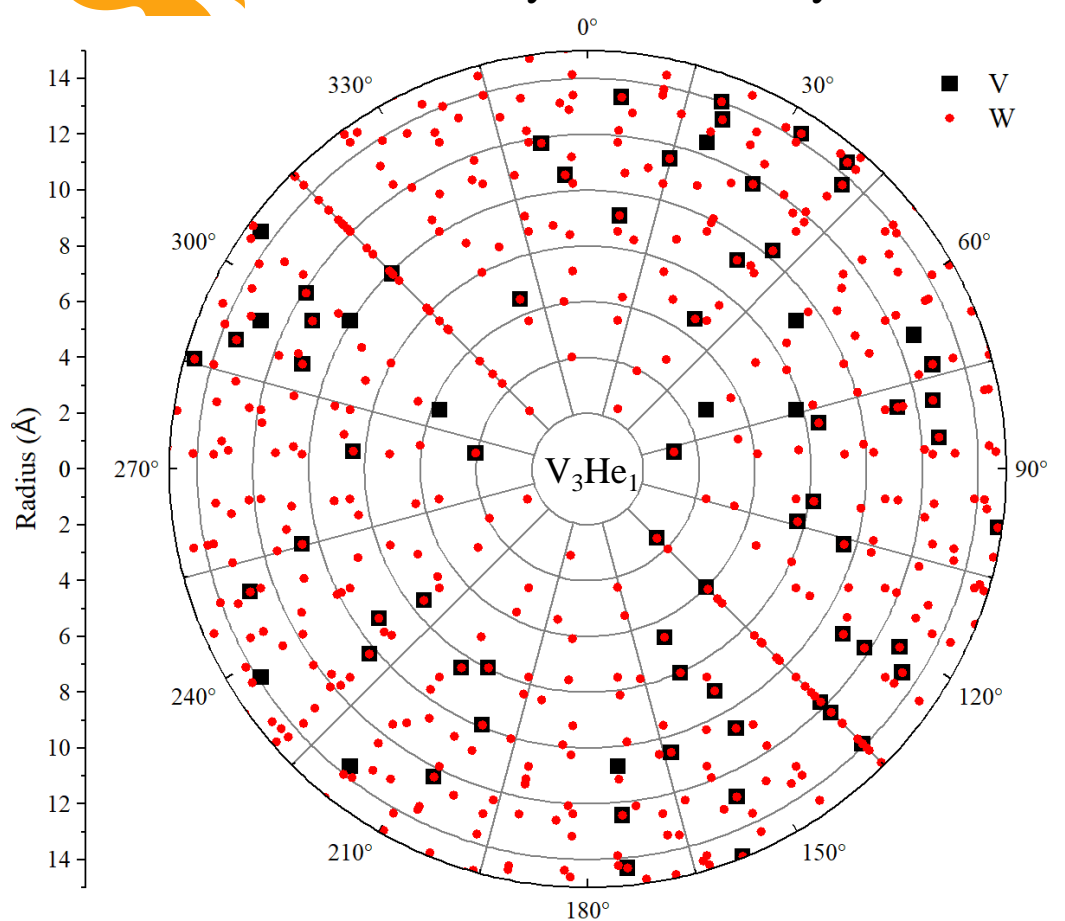
V₃ clusters exhibit extremely fast migration rates and serve as a key intermediate for vacancy-cluster nucleation and growth in W.

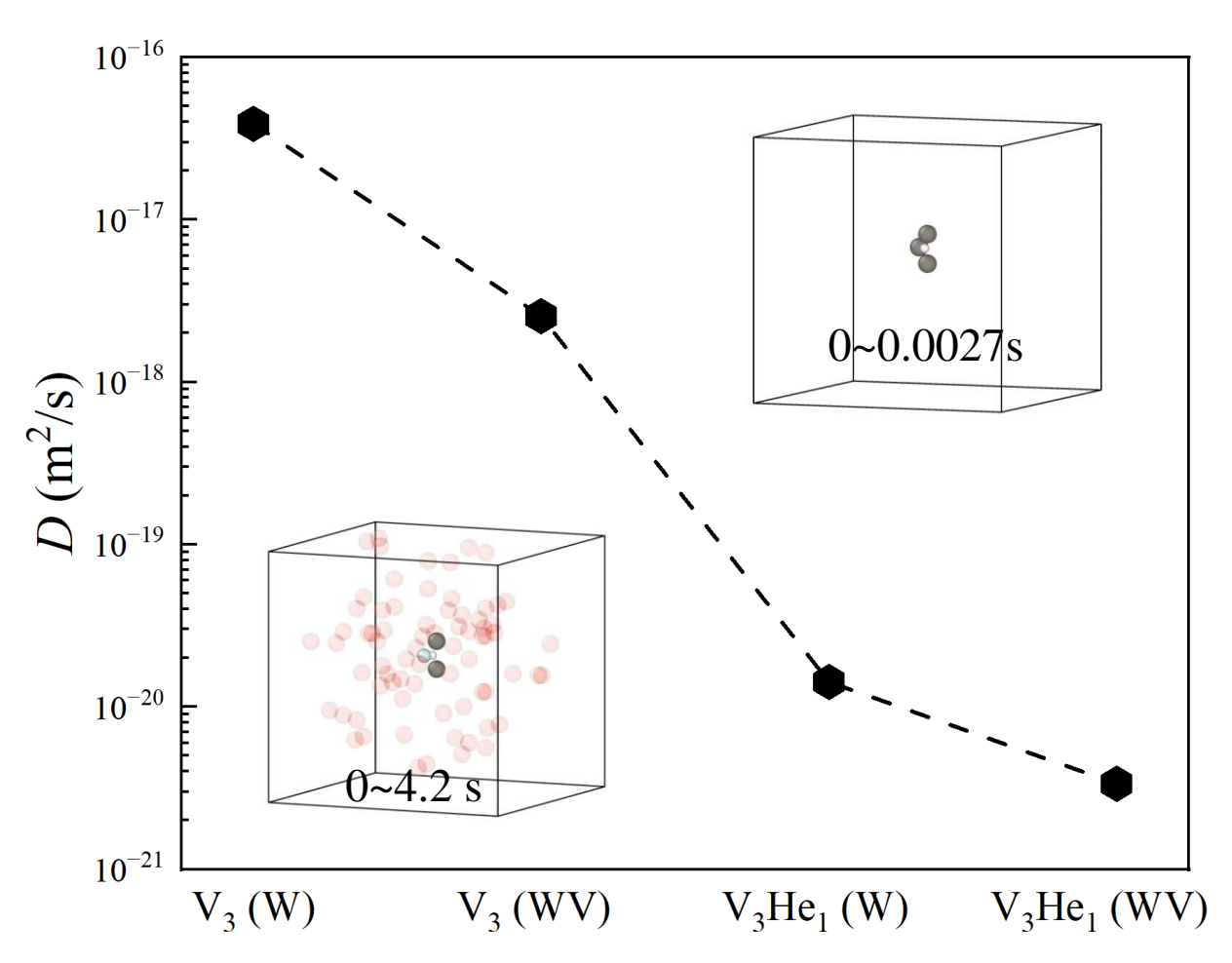
G. Wei, et al. Acta Materialia, 301 (2025) 121529.

The effect of V/He on the migration of V_3



5% V atoms are randomly and uniformly distributed in W





He and V effectively slow down V₃ migration and thus inhibit the nucleation and growth of vacancy clusters inside the W.



1. Simulation Validation

• The accurate tabGAP-pair potential for He-Mo-Nb-Ta-V-W proved effective for simulating irradiation damage and He diffusion.

2. The Critical Role of Vanadium (V)

- Controls Radiation Damage: The presence of V effectively controls radiation damage in refractory alloys.
- **Suppression Mechanism:** V suppresses He clustering at high temperatures (900-1500 K) and inhibits He self-trapping and the creation of vacancy traps (Frenkel pairs).
- **Trapping Sites:** V acts as a potent trapping site for mobile He atoms, creating stable, low-pressure "comfort sites" via elastic strain compensation.

3. Helium Diffusion & Defect Evolution

- **Inhibited Bubble Formation:** He atoms are less likely to form bubbles in V-containing alloys; diffusion is heavily influenced by lattice distortions.
- **He Release:** Unlike pure W where no release is detected, W-V binary alloys show significant He release (~20-30% at 1073K).
- Cluster Inhibition: He and V effectively slow down migration, inhibiting the nucleation and growth of vacancy clusters inside the W matrix.



Current published results

- •G.Wei, J.Byggmästar, J.Cui, K.Nordlund, J.Ren, F.Djurabekova, Revelaing the critical role of vanadium in radiation damage of tungsten-based alloys, Acta materialia, V.274, (1) 2024, 119991, DOI: 10.1016/j.actamat.2024.119991
- •G.Wei, J.Byggmästar, T.Sutinen, Z.Chen,F.Tuomisto, F.Djurabekova, Diffusion of helium in tungsten-basd refractory alloys by molecular dynamics simulations, Journal of Nuclear Materials, V.618, 2026, 156237, https://doi.org/10.1016/j.jnucmat.2025.156237
- •Z.Chen, E.Lu, K.Mizohata, A.Liski, X.An, T.Suhonen, A.Laukkanen, J.Lagerbom, A.Pasanen, A.Vaajoki, F.Tuomisto, Journal of Nuclear Materials, V.599,2024,155238, https://doi.org/10.1016/j.jnucmat.2024.155238
- •Z.Chen, G.Wei, K.Mizohata, E,Lu, , J.Byggmästar, F.Djurabekova, F.Tuomisto, Elemental diversity in high entropy alloy MoNbTaVW: complex He diffusion paths and improved radiation resistance, under review to Nature communications, https://doi.org/10.21203/rs.3.rs-7820411/v1 (pre-print)
- •G.Wei, J.Byggmästar, Z.Chen, F.Tuomisto, F.Djurabekova, Suppression of helium clustering in tungsten across temperature via dilute vanadium alloying, to be submitted shortly.







Thank you for your attention!